SUPPORTING INFORMATION

Influence of Ancillary Ligands on Photophysical Properties of Cyclometalated Organoplatinum(II) Complexes

Mozhgan Samandar,[a] Mohsen Golbon Haghighi,*[b]
S. Masoud Nabavizadeh,[a] Arno Pfitzner[c] and Mehdi Rashidi *[a]

[a] Professor Rashidi Laboratory of Organometallic Chemistry, Department of Chemistry, College of Sciences, Shiraz University, Shiraz 71467-13565, Iran

[b] Department of Chemistry, Shahid Beheshti University, Evin, Tehran 19839-69411, Iran

[c] Institut für Anorganische Chemie, Universität Regensburg, Universitätstarsse 31, Regensburg D-93053, Germany

E-mails: m_golbon@sbu.ac.ir (M.G.H.)

1. DFT and TDDFT calculations

1.1. Complex 1a

Table S1. Fragment contributions (%; from atomic orbital contributions) to the frontier orbitals of [Pt(*p*-Me-C_6H_4)(bhq)(PPh_3)], **1a** in CH_2Cl_2 solution.

Energies(eV)	number	Pt	PPh_3	Bhq	*P*-tol
-0.324	LUMO+6	4	78	16	2
-0.453	LUMO+5	5	85	8	2
-0.612	LUMO+4	13	80	6	1
-0.688	LUMO+3	6	87	6	1
-0.987	LUMO+2	4	91	4	1
-1.157	LUMO+1	3	9	87	1
-1.695	LUMO	3	2	94	1
-5.507	HOMO	24	5	10	61
-5.621	HOMO-1	30	3	67	0
-5.861	HOMO-2	82	2	6	10
-6.186	HOMO-3	42	1	41	16
-6.307	HOMO-4	18	3	7	72
-6.436	HOMO-5	11	57	30	2
-6.515	HOMO-6	54	1	39	6
-6.812	HOMO-7	49	6	44	1
-6.912	HOMO-8	2	93	3	2
-6.996	HOMO-9	8	85	5	2
-7.097	HOMO-10	6	87	4	3
-7.162	HOMO-11	4	94	2	0

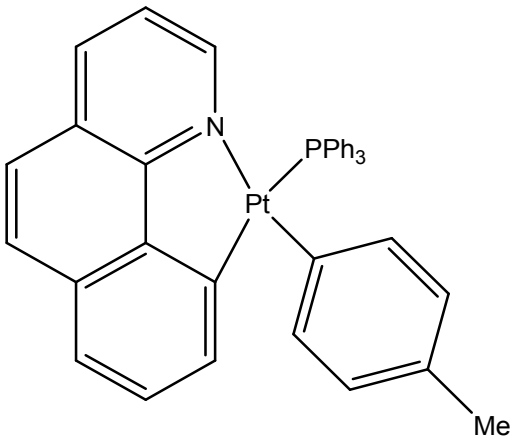

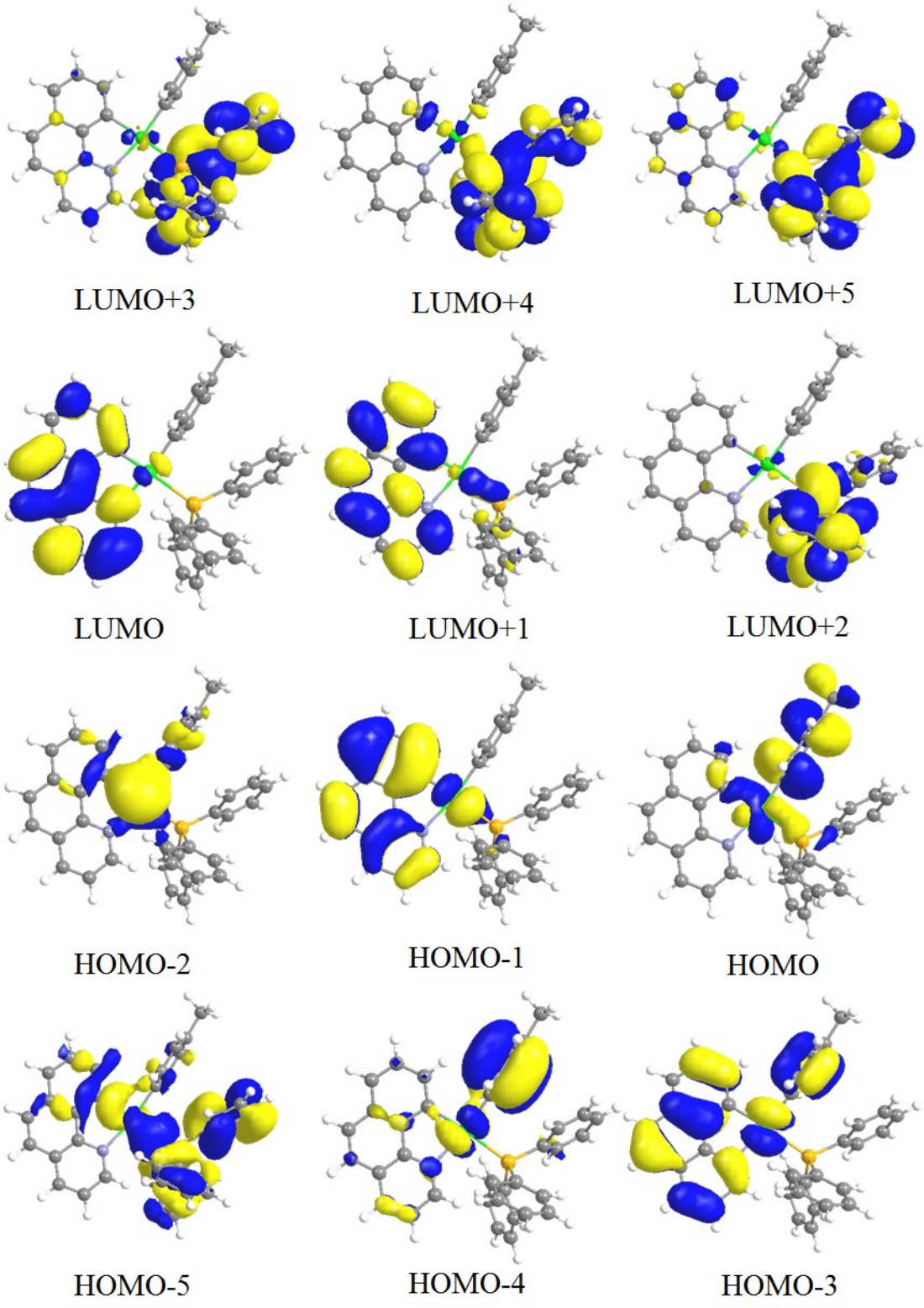

Figure S1. Qualitative frontier molecular orbitals for complex **1a.**

Table S2. Fragment contributions (%; from atomic orbital contributions) to the frontier orbitals of [Pt(*p*-Me-C_6H_4)(bhq)(PPh_3)], **1a** in gas phase.

Energies(eV)	number	Pt	PPh_3	Bhq	*P*-tol
-0.250	LUMO+6	3	89	7	1
-0.316	LUMO+5	5	90	4	1
-0.502	LUMO+4	11	82	5	2
-0.624	LUMO+3	2	92	5	1
-0.918	LUMO+2	3	84	12	1
-0.962	LUMO+1	4	30	65	1
-1.756	LUMO	2	1	96	1
-5.077	HOMO	23	4	28	45
-5.106	HOMO-1	21	4	54	21
-5.492	HOMO-2	79	2	9	10
-5.779	HOMO-3	24	3	19	54
-5.881	HOMO-4	42	1	28	29
-6.159	HOMO-5	65	2	27	6
-6.240	HOMO-6	11	55	32	2
-6.558	HOMO-7	39	4	57	0
-6.708	HOMO-8	2	94	2	2
-6.857	HOMO-9	29	30	19	22
-7.005	HOMO-10	8	61	12	19
-7.084	HOMO-11	11	65	9	15

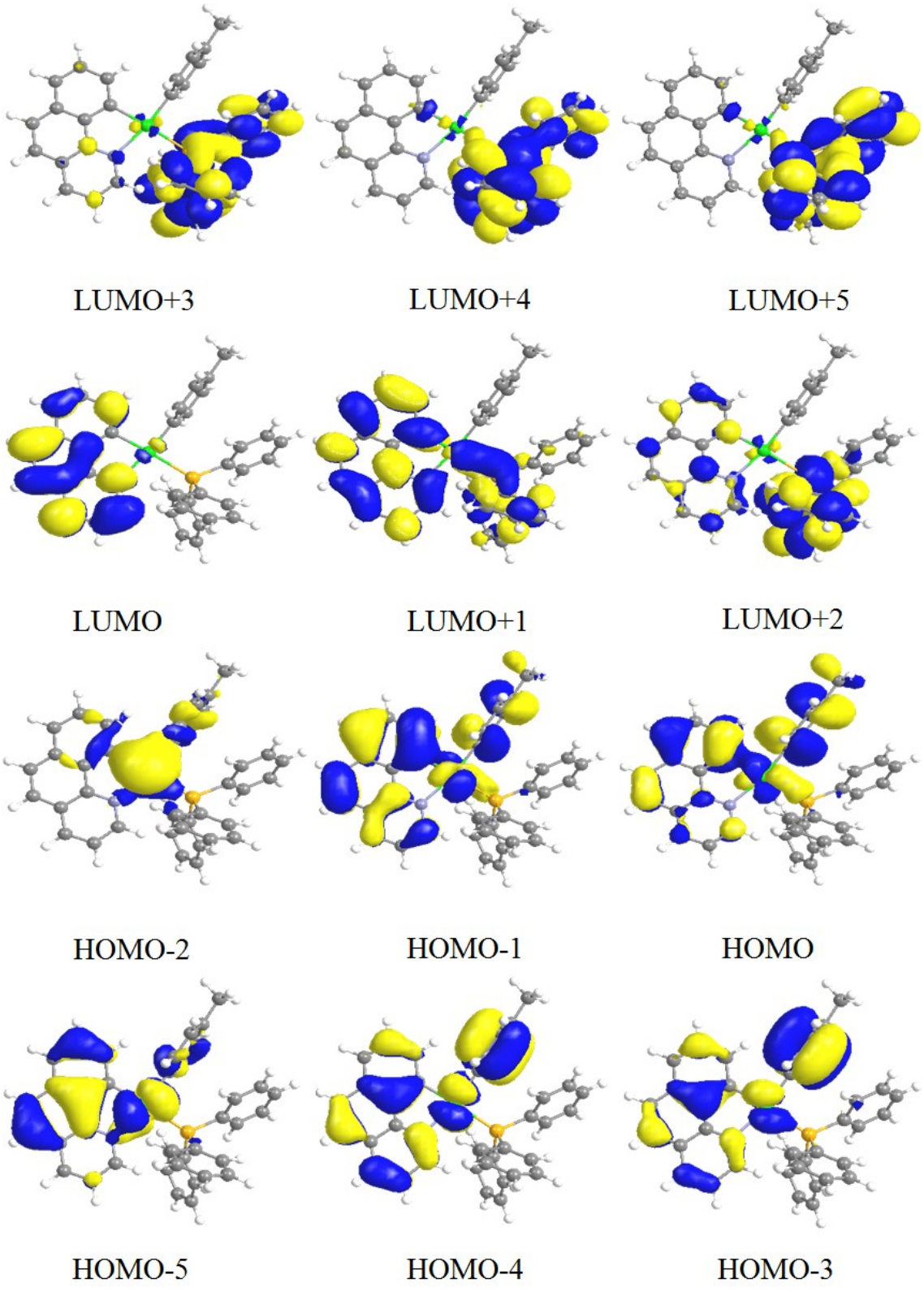

Figure S2. Qualitative frontier molecular orbitals for complex **1a** in gas phase**.**

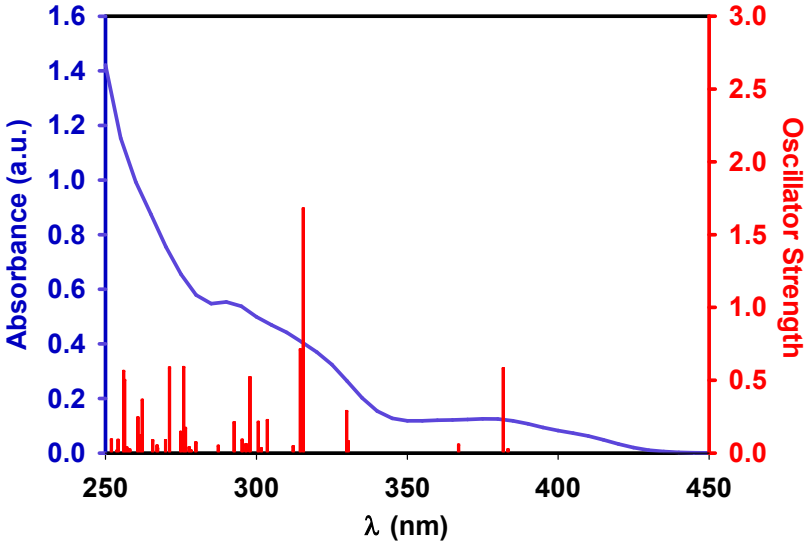

Figure S3. Experimental UV-vis spectra in CH_2Cl_2 (10^{-5} M) at 298 K and calculated absorption spectra, showing by bars, in CH_2Cl_2 for the complex **1a**.

Table S3. Selected vertical singlet excitations of **1a** from TDDFT calculations at the ground state geometry in CH_2Cl_2 solution (10^{-5}).

state	Monoexcitations[a]	Δ E/eV	λ_{cal}/nm	oscillator strength		main character
S1	H→L (73%) H-1→L (19%)	3.238	383	0.0022		MLCT/LC/LLCT
S2	H-1→L (75%) H→L (19%)	3.251	381	0.0579	19%	MLCT/LC/LLCT
S3	H-2→L (92%)	3.382	366	0.0054		MLCT/LLCT
S4	H→L+1 (77%) H-3→L (10%)	3.757	330	0.0078		MLCT/LC/LLCT
S5	H-3→L (41%) H-1→L+1 (30%) H→L+1 (17%)	3.763	329	0.0285		MLCT/LC/LLCT
S6	H-1→L+1 (33%) H-2→L+1 (25%) H-3→L (16%) H-6→L (14%)	3.933	315	0.1677		MLCT/LC/LLCT
S7	H-2→L+1 (68%) H-1→L+1 (13%)	3.946	314	0.0708		MLCT/LC/LLCT
S8	H→L+2 (94%)	3.976	312	0.0043		MLCT/LLCT
S9	H-4→L (35%) H-6→L (27%) H-3→L (18%)	4.088	303	0.0223		MLCT/LC/LLCT
S12	H-4→L (39%) H-3→L+1 (16%) H-6→L (15%)	4.167	298	0.052		MLCT/LC/LLCT
S14	H→L+3 (60%)	4.202	295	0.0088		MLCT/LLCT

	H-2→L+2 (18%) H→L+4 (14%)					
S15	H-3→L+1 (29%) H-7→L (24%) H-6→L (18%) H-4→L (10%)	4.240	292	0.0208		MLCT/LC/LLCT
S16	H→L+4 (72%) H→L+3 (21%)	4.318	287	0.0046		MLCT/LLCT
S20	H-2→L+3 (45%) H-2→L+4 (19%) H→L+5 (16%)	4.487	276	0.017		MLCT/LLCT
S21	H-6→L+1 (38%) H-7→L (22%) H-2→L+3 (12%)	4.497	275	0.059		MLCT/LC/LLCT

Table S4. Lowest-energy vertical triplet excitations of **1a** from TDDFT calculations in gas phase.

state	Monoexcitations[a]	Δ E/eV	λ_{cal}/nm	main character
T1	H-1→L (47%) H→L (25%)	1.935	641	MLCT/LC/LLCT
T2	H-1→L+1 (28%) H-1→L (15%) H→L+1 (13%) H-4→L (10%)	2.709	458	MLCT/LC/LLCT
T3	H→L (58%) H-1→L (33%)	2.780	446	MLCT/LC/LLCT
T4	H-4→L (32%) H-3→L (22%) H-1→L+1 (17%)	2.864	433	MLCT/LC/LLCT
T5	H-2→L (91%)	2.941	422	MLCT/LC/LLCT

1.2. Complex 1b

Table S5. Fragment contributions (%; from atomic orbital contributions) to the frontier orbitals of [Pt(*p*-Me-C_6H_4)(bhq)(PPh_2Me)], **1b** in CH_2Cl_2 solution.

Energies(eV)	number	Pt	PPh_2Me	Bhq	*P*-tol
-0.155	LUMO+6	4	45	48	3
-0.286	LUMO+5	6	67	25	2
-0.422	LUMO+4	5	85	8	1
-0.604	LUMO+3	9	83	7	1
-0.866	LUMO+2	3	93	2	2
-1.152	LUMO+1	3	7	89	1
-1.685	LUMO	3	2	94	1
-5.550	HOMO	25	6	9	60
-5.618	HOMO-1	29	3	68	0
-5.865	HOMO-2	83	2	7	8
-6.192	HOMO-3	46	1	46	7
-6.357	HOMO-4	15	3	2	80
-6.513	HOMO-5	45	8	40	7
-6.599	HOMO-6	22	41	35	2
-6.809	HOMO-7	50	6	43	1
-7.044	HOMO-8	1	96	2	1
-7.101	HOMO-9	2	95	2	1
-7.154	HOMO-10	5	79	7	9
-7.278	HOMO-11	18	38	23	21

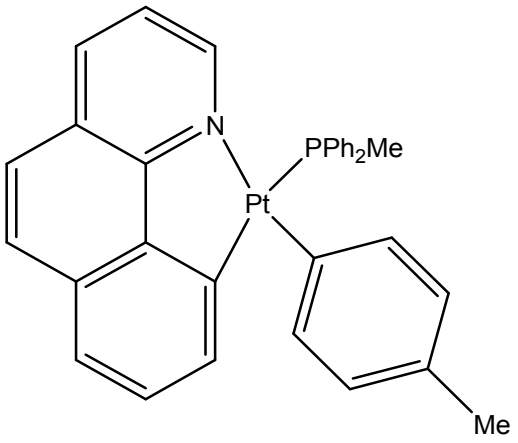

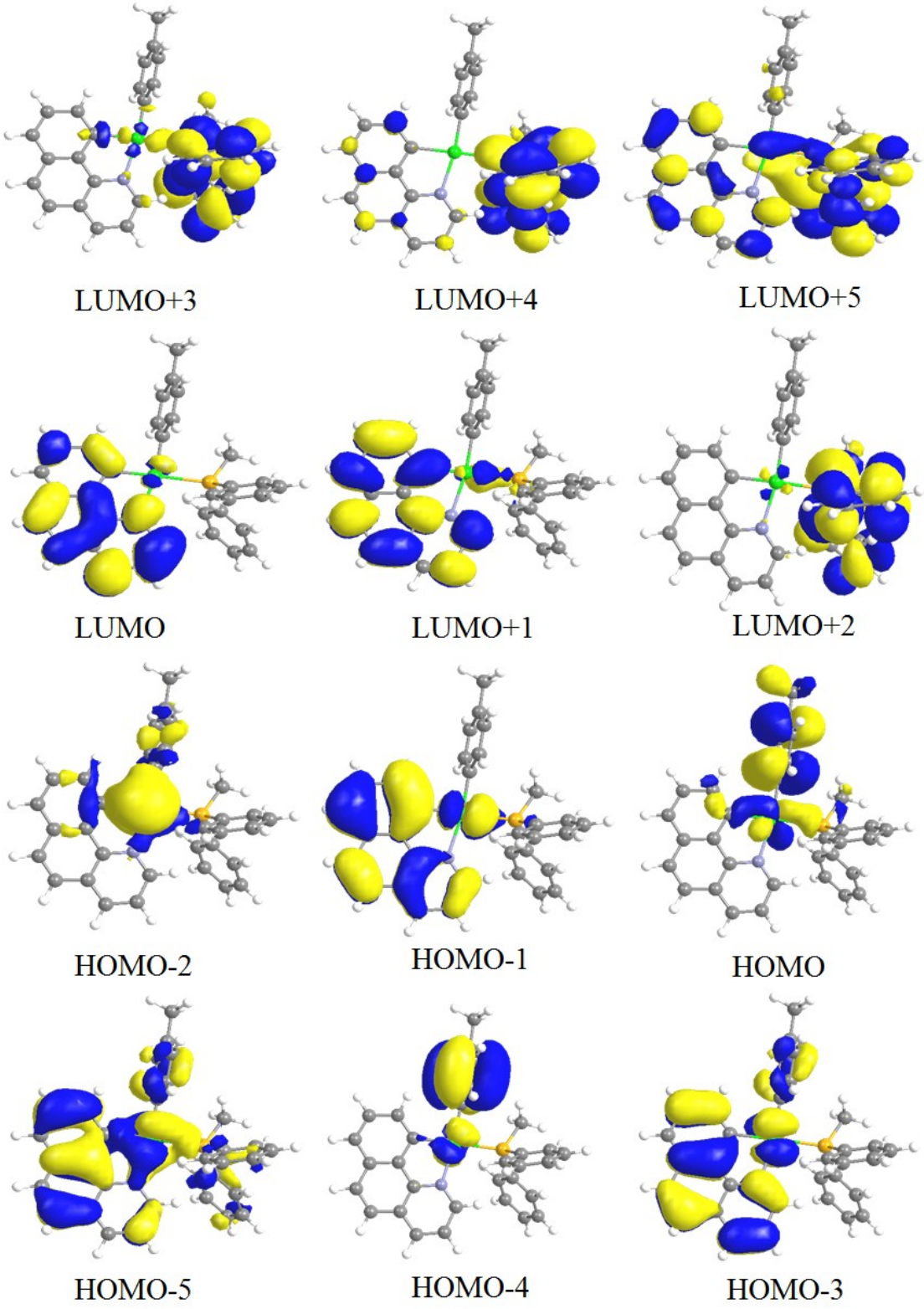

Figure S4. Qualitative frontier molecular orbitals for complex **1b.**

Table S6. Fragment contributions (%; from atomic orbital contributions) to the frontier orbitals of [Pt(*p*-Me-C_6H_4)(bhq)(PPh_2Me)], **1b** in gas phase.

Energies(eV)	number	Pt	PPh_2Me	Bhq	*P*-tol
0.089	LUMO+6	4	12	80	4
-0.249	LUMO+5	3	94	3	0
-0.414	LUMO+4	6	89	5	1
-0.561	LUMO+3	5	88	6	1
-0.858	LUMO+2	2	93	4	1
-0.967	LUMO+1	4	14	81	1
-1.772	LUMO	2	1	96	1
-5.113	HOMO	20	3	77	0
-5.163	HOMO-1	23	5	10	62
-5.511	HOMO-2	80	2	9	9
-5.833	HOMO-3	44	1	36	19
-5.937	HOMO-4	23	2	9	66
-6.187	HOMO-5	64	2	28	6
-6.462	HOMO-6	16	41	41	2
-6.573	HOMO-7	40	3	57	0
-6.988	HOMO-8	21	17	23	39
-7.055	HOMO-9	1	93	3	3
-7.100	HOMO-10	1	95	2	2
-7.174	HOMO-11	50	19	13	18

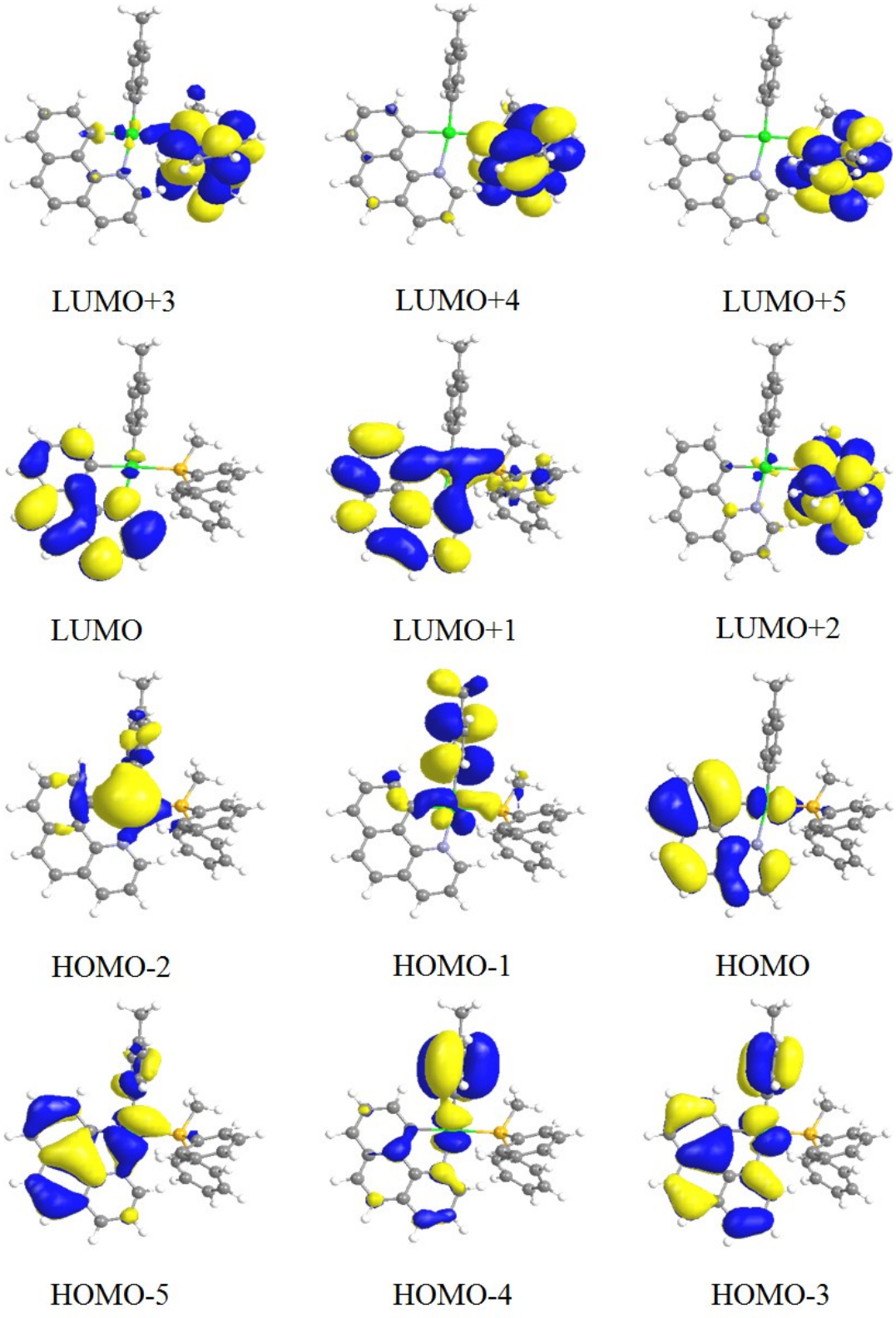

Figure S5. Qualitative frontier molecular orbitals for complex **1b** in gas phase**.**

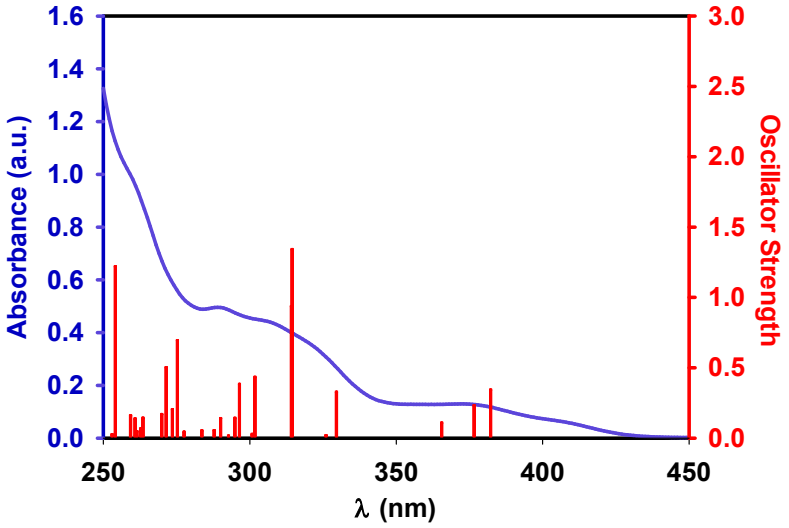

Figure S6. Experimental UV-vis spectra in CH_2Cl_2 (10^{-5} M) at 298 K and calculated absorption spectra, showing by bars, in CH_2Cl_2 for the complex **1b**.

Table S7. Selected vertical singlet excitations of **1b** from TDDFT calculations at the ground state geometry in CH_2Cl_2 solution (10^{-5}).

state	Monoexcitations[a]	Δ E/eV	λ_{cal}/nm	oscillator strength	main character
S1	H-1→L (79%) H→L (16%)	3.248	382	0.0342	MLCT/LC/LLCT
S2	H→L (73%) H-1→L (14%) H-2→L (11%)	3.296	376	0.0231	MLCT/LC/LLCT
S3	H-2→L (87%)	3.396	365	0.0107	MLCT
S4	H-3→L (50%) H-1→L+1 (38%)	3.766	329	0.0326	MLCT/LC
S5	H-2→L+1 (38%) H-1→L+1 (26%) H-3→L (19%)	3.807	314	0.1341	MLCT/LC
S7	H-2→L+1 (56%) H-1→L+1 (19%)	3.950	314	0.0935	MLCT/LC
S8	H-5→L (38%) H-4→L (22%) H-3→L (13%)	4.113	301	0.0432	MLCT/LC/LLCT
S10	H-6→L (28%) H-4→L (28%) H-3→L+1 (26%)	4.186	296	0.0382	MLCT/LC/LLCT
S11	H-6→L (63%)	4.208	295	0.0141	MLCT/LC/LLCT
S13	H-4→L (29%) H-5→L (23%) H-3→L+1 (19%) H-7→L (16%)	4.279	290	0.014	MLCT/LC/LLCT
S17	H-5→L+1 (37%) H-7→L (22%)	4.508	275	0.069	MLCT/LC

	H-3→L+1 (10%)				
S18	H-2→L+3 (80%)	4.536	273	0.0203	MLCT
S19	H-7→L (28%) H-1→L+4 (10%) H-1→L+5 (10%)	4.571	271	0.0502	MLCT/LC/LLCT
S20	H→L+4 (72%) H→L+5 (11%)	4.597	270	0.017	MLCT/LC/LLCT
S21	H-6→L+1 (18%) H-4→L+1 (63%)	4.708	263	0.014	MLCT/LC/LLCT
S25	H-1→L+4 (53%) H-5→L+1 (10%) H-4→L+1 (10%)	4.757	261	0.014	MLCT/LC/LLCT
S27	H-2→L+4 (47%) H-2→L+5 (18%)	4.785	259	0.016	MLCT

Table S8. Lowest-energy vertical triplet excitations of **1b** from TDDFT calculations in gas phase.

state	Monoexcitations[a]	Δ E/eV	λ_{cal}/nm	main character
T1	H→L (71%) H-3→L (10%)	1.935	641	MLCT/LC/LLCT
T2	H→L+1 (41%) H→L (24%) H-3→L (19%)	2.706	458	MLCT/LC/LLCT
T3	H-1→L (59%) H→L+1 (18%) H-3→L (12%)	2.818	440	MLCT/LC/LLCT
T4	H-3→L (28%) H-1→L (24%) H-2→L (17%) H→L+1 (17%)	2.873	432	MLCT/LC/LLCT
T5	H-2→L (77%) H-1→L (13%)	2.950	420	MLCT/LC/LLCT

1.3. Complex 1c

Table S9. Fragment contributions (%; from atomic orbital contributions) to the frontier orbitals of [Pt(*p*-Me-C_6H_4)(bhq)($PPhMe_2$)], **1c** in CH_2Cl_2 solution.

Energies(eV)	number	Pt	$PPhMe_2$	Bhq	*P*-tol
0.373	LUMO+6	21	24	31	24
0.350	LUMO+5	16	8	14	62
-0.222	LUMO+4	8	24	63	5
-0.341	LUMO+3	6	79	14	1
-0.710	LUMO+2	4	90	5	1
-1.154	LUMO+1	4	6	89	1
-1.696	LUMO	3	2	94	1
-5.536	HOMO	24	6	10	60
-5.611	HOMO-1	30	3	67	0
-5.863	HOMO-2	84	1	7	8
-6.178	HOMO-3	49	0	44	7
-6.346	HOMO-4	14	2	2	82
-6.515	HOMO-5	50	1	42	7
-6.699	HOMO-6	16	39	43	2
-6.814	HOMO-7	51	4	44	1
-7.071	HOMO-8	2	95	2	1
-7.141	HOMO-9	11	58	19	12
-7.393	HOMO-10	22	16	28	34
-7.556	HOMO-11	52	4	14	30

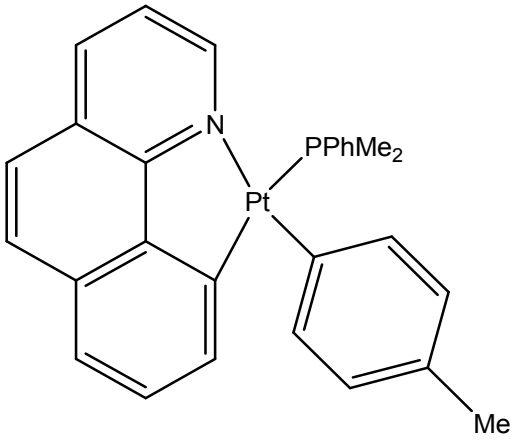

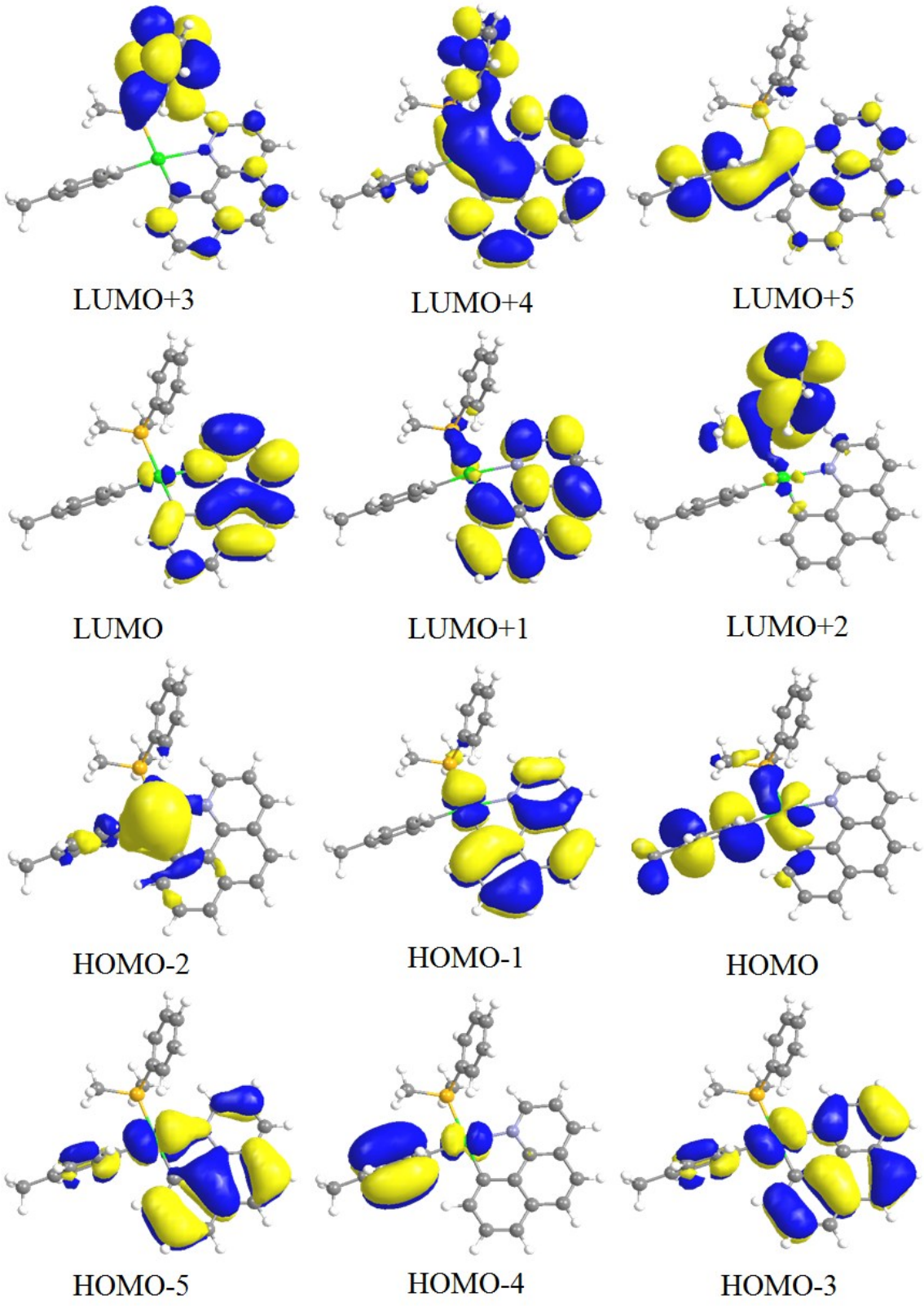

Figure S7. Qualitative frontier molecular orbitals for complex **1c.**

Table S10. Fragment contributions (%; from atomic orbital contributions) to the frontier orbitals of [Pt(*p*-Me-C_6H_4)(bhq)($PPhMe_2$)], **1c** in gas phase.

Energies(eV)	number	Pt	$PPhMe_2$	Bhq	*P*-tol
-0.384	LUMO+3	2	93	4	1
-0.780	LUMO+2	1	93	5	1
-0.992	LUMO+1	5	12	82	1
-1.818	LUMO	2	2	96	0
-5.134	HOMO	21	3	71	5
-5.174	HOMO-1	22	5	15	58
-5.538	HOMO-2	80	2	9	9
-5.845	HOMO-3	43	1	34	22
-5.948	HOMO-4	26	1	11	62
-6.209	HOMO-5	63	1	30	6
-6.576	HOMO-6	29	16	54	1
-6.649	HOMO-7	24	22	52	2
-7.011	HOMO-8	20	21	23	37

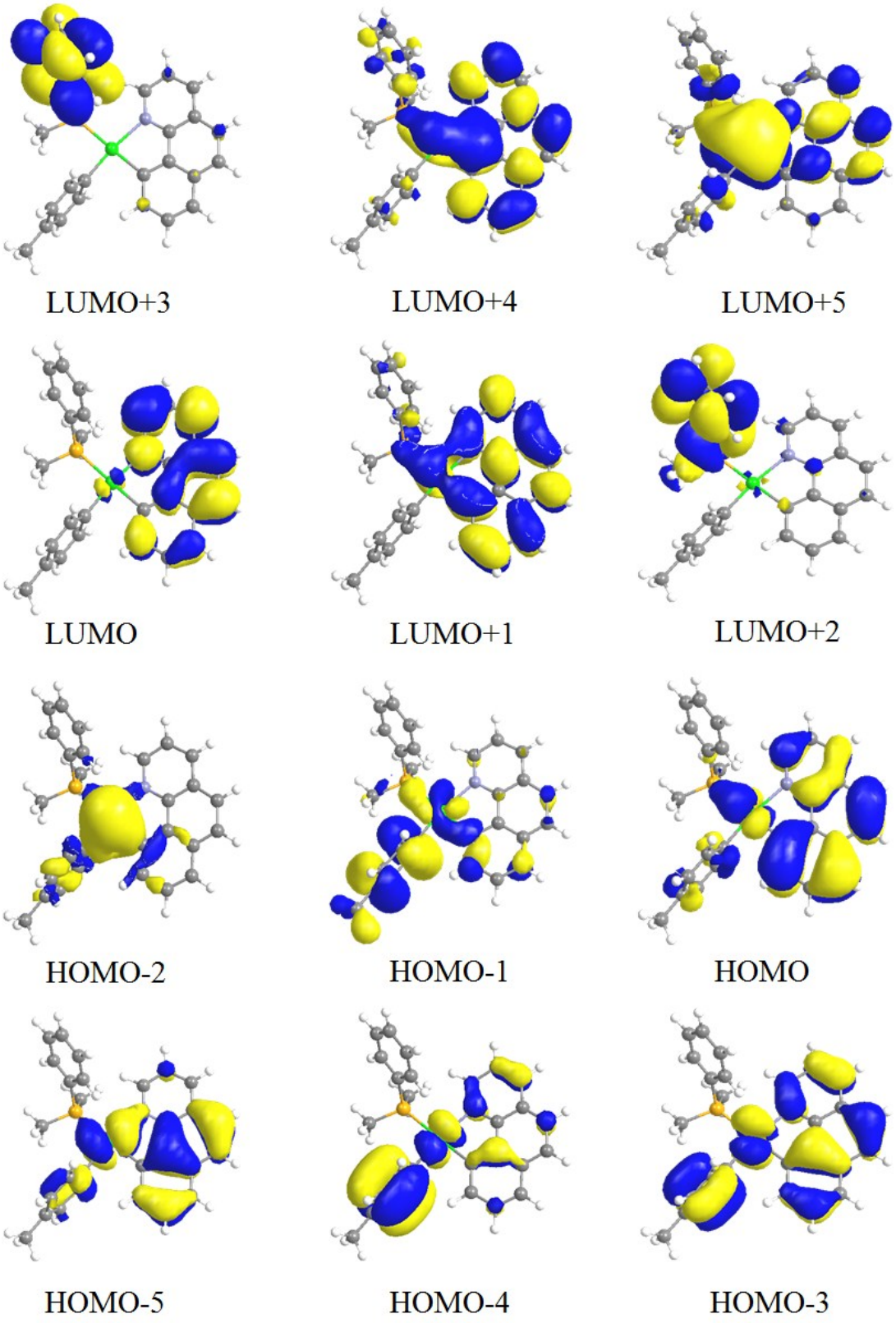

Figure S8. Qualitative frontier molecular orbitals for complex **1c** in gas phase.

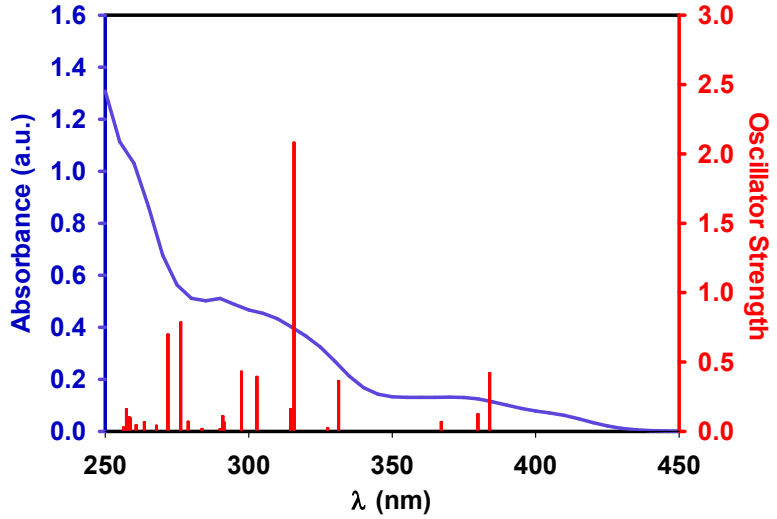

Figure S9. Experimental UV-vis spectra in CH_2Cl_2 (10^{-5} M) at 298 K and calculated absorption spectra, showing by bars, in CH_2Cl_2 for the complex **1c**.

Table S11. Selected vertical singlet excitations of **1c** from TDDFT calculations at the ground state geometry in CH_2Cl_2 solution (10^{-5}).

state	Monoexcitations[a]	Δ E/eV	λ_{cal}/nm	oscillator strength	main character
S1	H-1→L (83%) H→L (12%)	3.233	383	0.0416	MLCT/LC/LLCT
S2	H→L (78%) H-1→L (11%)	3.268	379	0.0121	MLCT/LC/LLCT
S3	H-2→L (89%)	3.381	367	0.0064	MLCT
S4	H-3→L (53%) H-1→L+1 (37%)	3.747	331	0.036	MLCT/LC
S6	H-1→L+1 (46%) H-3→L (25%) H-5→L (17%)	3.930	315	0.208	MLCT/LC
S7	H-2→L+1 (90%)	3.945	314	0.0156	MLCT
S8	H-5→L (44%) H-4→L (24%) H-3→L (13%)	4.098	303	0.039	MLCT/LC/LLCT
S9	H-4→L (40%) H-3→L+1 (35%) H-7→L (14%)	4.172	297	0.0426	MLCT/LC/LLCT
S11	H-6→L (23%) H-4→L (23%) H-5→L (20%) H-3→L+1 (14%) H-7→L (12%)	4.265	291	0.011	MLCT/LC/LLCT
S15	H-5→L+1 (47%) H-7→L (22%) H-3→L+1 (11%)	4.491	276	0.078	MLCT/LC
S16	H-7→L (35%)	4.564	272	0.0695	MLCT/LC/LLCT

	H-1→L+4 (21%) H-5→L+1 (14%) H-1→L+3 (10%)				
S26	H-2→L+3 (80%)	4.955	250	0.1986	MLCT

Table S12. Lowest-energy vertical triplet excitations of **1c** from TDDFT calculations in gas phase.

state	Monoexcitations[a]	Δ E/eV	λ_{cal}/nm	main character
T1	H→L (66%)	1.926	644	MLCT/LC
T2	H→L+1 (33%) H→L (27%) H-3→L (22%)	2.690	461	MLCT/LC/LLCT
T3	H-1→L (73%)	2.795	443	MLCT/LC/LLCT
T4	H-3→L (32%) H→L+1 (30%)	2.844	436	MLCT/LC/LLCT
T5	H-2→L (80%) H-1→L (11%)	2.929	423	MLCT/LC/LLCT

1.4. Complex 2a

Table S13. Fragment contributions (%; from atomic orbital contributions) to the frontier orbitals of [Pt(C_6H_5)(bhq)(PPh_2Me)], **2a** in CH_2Cl_2 solution.

Energies(eV)	number	Pt	PPh_2Me	Bhq	C_6H_5
-0.161	LUMO+6	4	47	46	3
-0.285	LUMO+5	6	63	28	3
-0.427	LUMO+4	5	86	7	2
-0.614	LUMO+3	10	82	6	2
-0.867	LUMO+2	3	94	2	1
-1.156	LUMO+1	4	6	89	1
-1.689	LUMO	3	2	94	1
-5.624	HOMO	29	3	67	1
-5.711	HOMO-1	31	6	12	51
-5.876	HOMO-2	82	2	6	10
-6.206	HOMO-3	44	1	48	7
-6.398	HOMO-4	16	4	4	76
-6.523	HOMO-5	41	11	39	9
-6.608	HOMO-6	26	38	34	2
-6.815	HOMO-7	50	6	43	1
-7.047	HOMO-8	1	97	1	1
-7.107	HOMO-9	2	95	2	1
-7.160	HOMO-10	5	82	6	7
-7.292	HOMO-11	16	38	25	21
-7.506	HOMO-12	12	29	35	24

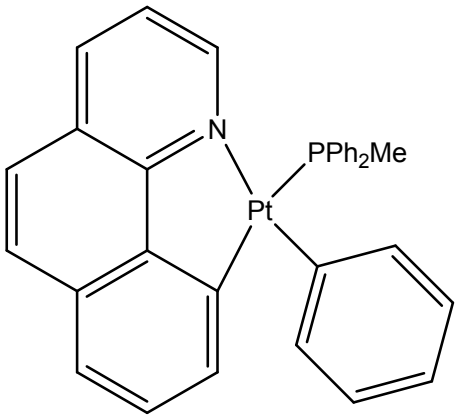

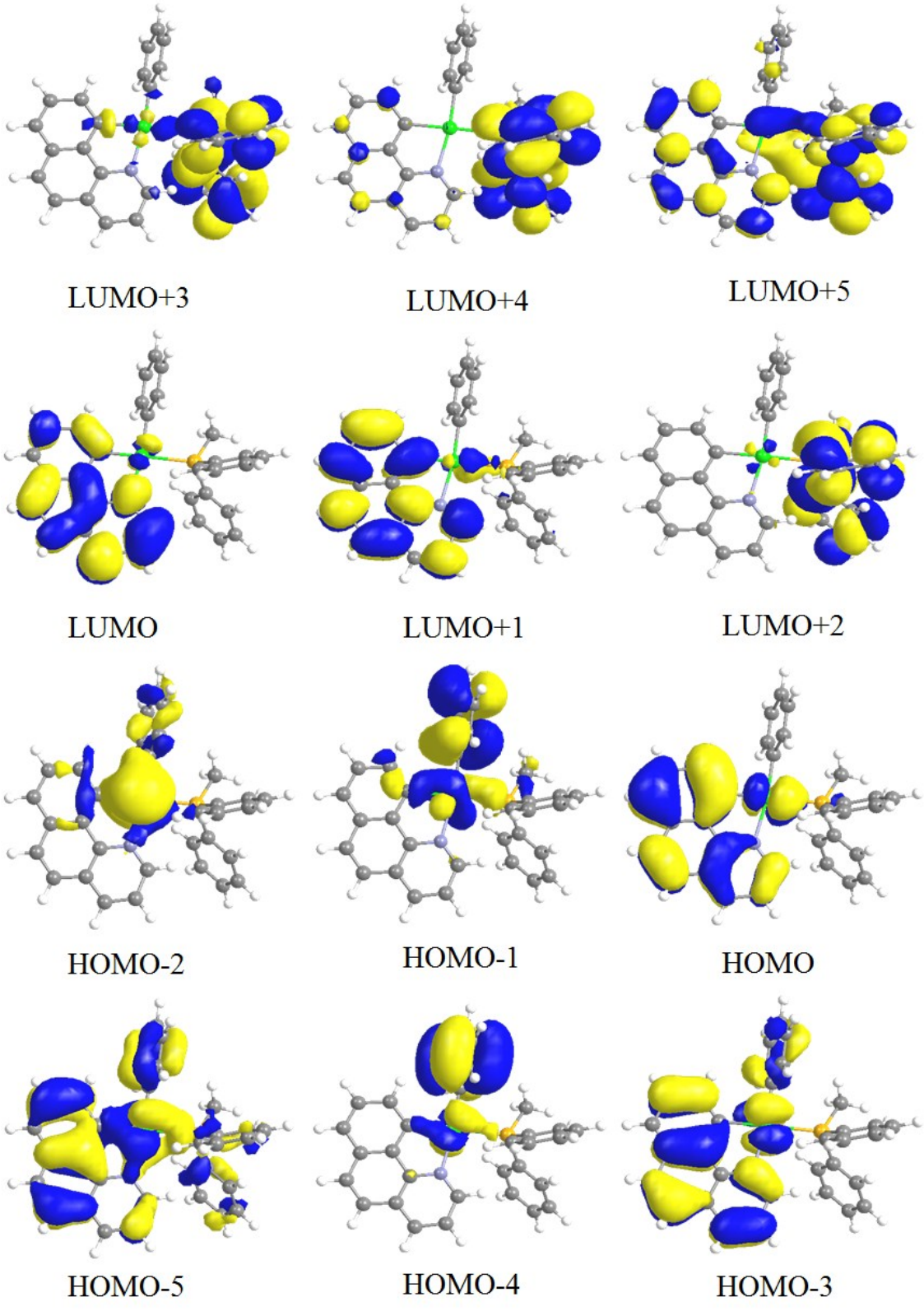

Figure S10. Qualitative frontier molecular orbitals for complex **2a.**

Table S14. Fragment contributions (%; from atomic orbital contributions) to the frontier orbitals of [Pt(C_6H_5)(bhq)(PPh_2Me)], **2a** in gas phase.

Energies(eV)	number	Pt	PPh_2Me	Bhq	C_6H_5
0.078	LUMO+6	4	12	80	4
-0.255	LUMO+5	3	94	3	0
-0.427	LUMO+4	6	88	5	1
-0.575	LUMO+3	5	88	6	1
-0.866	LUMO+2	2	93	4	1
-0.979	LUMO+1	4	13	82	1
-1.784	LUMO	2	1	96	1
-5.126	HOMO	20	3	77	0
-5.319	HOMO-1	28	6	11	55
-5.532	HOMO-2	80	2	8	10
-5.853	HOMO-3	44	1	39	16
-5.970	HOMO-4	20	2	8	70
-6.206	HOMO-5	64	2	27	7
-6.476	HOMO-6	16	41	41	2
-6.586	HOMO-7	40	3	57	0
-7.017	HOMO-8	17	19	25	39
-7.066	HOMO-9	1	95	2	2
-7.109	HOMO-10	2	95	2	1
-7.216	HOMO-11	4	83	7	6

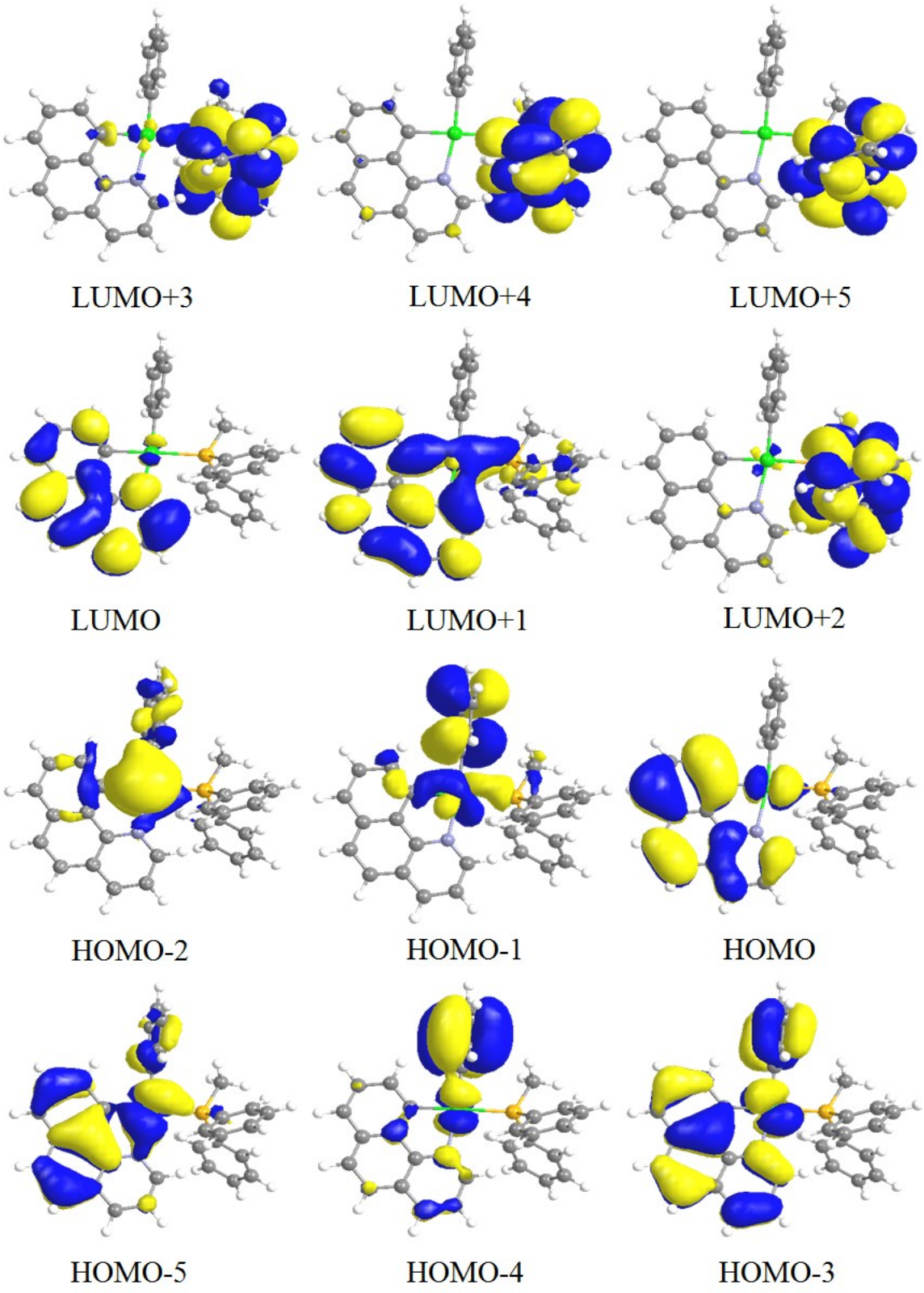

Figure S11. Qualitative frontier molecular orbitals for complex **2a** in gas phase.

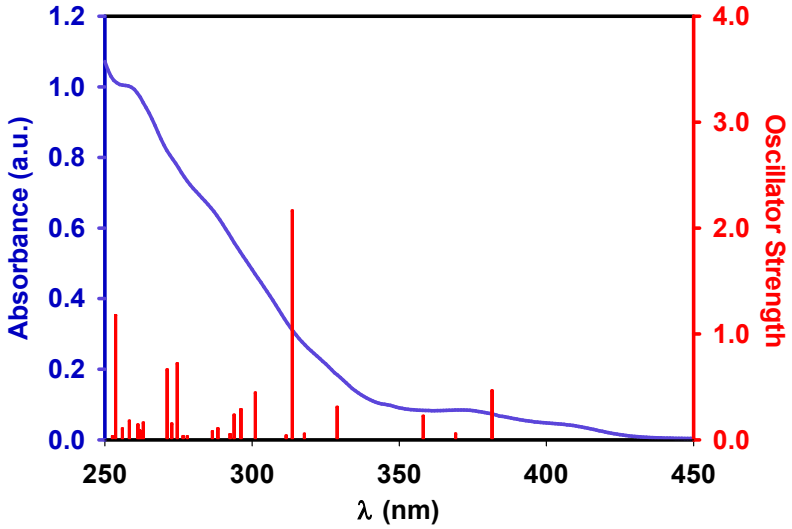

Figure S12. Experimental UV-vis spectra in CH_2Cl_2 (10^{-5} M) at 298 K and calculated absorption spectra, showing by bars, in CH_2Cl_2 for the complex **2a**.

Table S15. Selected vertical singlet excitations of **2a** from TDDFT calculations at the ground state geometry in CH_2Cl_2 solution (10^{-5}).

state	Monoexcitations[a]	Δ E/eV	λ_{cal}/nm	oscillator strength	main character
S1	H→L (93%)	3.254	381	0.0461	MLCT/LC
S2	H-2→L (62%) H-1→L (36%)	3.363	369	0.0054	MLCT/LC/LLCT
S3	H-1→L (60%) H-2→L (36%)	3.466	358	0.0222	MLCT/LC/LLCT
S4	H-3→L (50%) H→L+1 (42%)	3.774	328	0.031	MLCT/LC
S6	H→L+1 (43%) H-3→L (31%) H-5→L (15%)	3.957	313	0.216	MLCT/LC/LLCT
S8	H-5→L (43%) H-4→L (24%) H-3→L (12%)	4.122	301	0.044	MLCT/LC/LLCT
S9	H-6→L (54%) H-3→L+1 (19%) H-4→L (14%)	4.189	296	0.0285	MLCT/LC/LLCT
S10	H-6→L (30%) H→L+2 (22%) H-3→L+1 (17%) H-7→L (12%)	4.223	294	0.0232	MLCT/LC/LLCT
S13	H-4→L (40%) H-5→L (27%) H-3→L+1 (13%) H-7→L (10%)	4.303	288	0.0103	MLCT/LC/LLCT
S17	H-5→L+1 (39%) H-7→L (16%)	4.519	274	0.072	MLCT/LC/LLCT

	H-3→L+1 (10%)				
S26	H-2→L+3 (80%)	4.955	250	0.1986	MLCT/LLCT

Table S16. Lowest-energy vertical triplet excitations of **2a** from TDDFT calculations in gas phase.

state	Monoexcitations[a]	Δ E/eV	λ_{cal}/nm	main character
T1	H→L (71%) H-3→L (10%)	1.935	641	MLCT/LC/LLCT
T2	H→L+1 (43%) H→L (24%) H-3→L (19%)	2.708	458	MLCT/LC/LLCT
T3	H-3→L (39%) H→L+1 (33%) H-1→L (11%)	2.847	435	MLCT/LC/LLCT
T4	H-2→L (61%) H-1→L (33%)	2.909	426	MLCT/LC/LLCT
T5	H-1→L (54%) H-2→L (35%)	3.020	411	MLCT/LC/LLCT

1.5. Complex 2b

Table S17. Fragment contributions (%; from atomic orbital contributions) to the frontier orbitals of [Pt(*p*-F-C_6H_4)(bhq)(PPh_2Me)], **2b** in CH_2Cl_2 solution.

Energies(eV)	number	Pt	PPh_2Me	Bhq	*p*-F-C_6H_4
-0.305	LUMO+5	6	62	27	5
-0.438	LUMO+4	5	84	9	2
-0.622	LUMO+3	9	82	7	2
-0.885	LUMO+2	3	93	2	2
-1.173	LUMO+1	4	7	89	0
-1.709	LUMO	3	2	94	1
-5.645	HOMO	29	3	67	1
-5.664	HOMO-1	25	6	11	58
-5.924	HOMO-2	84	2	7	7
-6.232	HOMO-3	43	1	51	5
-6.537	HOMO-4	48	12	31	9
-6.630	HOMO-5	27	36	34	3
-6.653	HOMO-6	6	7	11	76
-6.847	HOMO-7	47	6	41	6
-7.059	HOMO-8	1	97	2	0
-7.116	HOMO-9	2	96	2	0
-7.180	HOMO-10	4	87	5	4
-7.335	HOMO-11	16	46	26	12
-7.539	HOMO-12	32	18	27	23

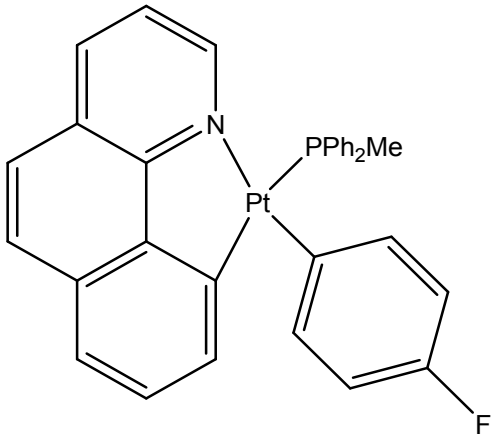

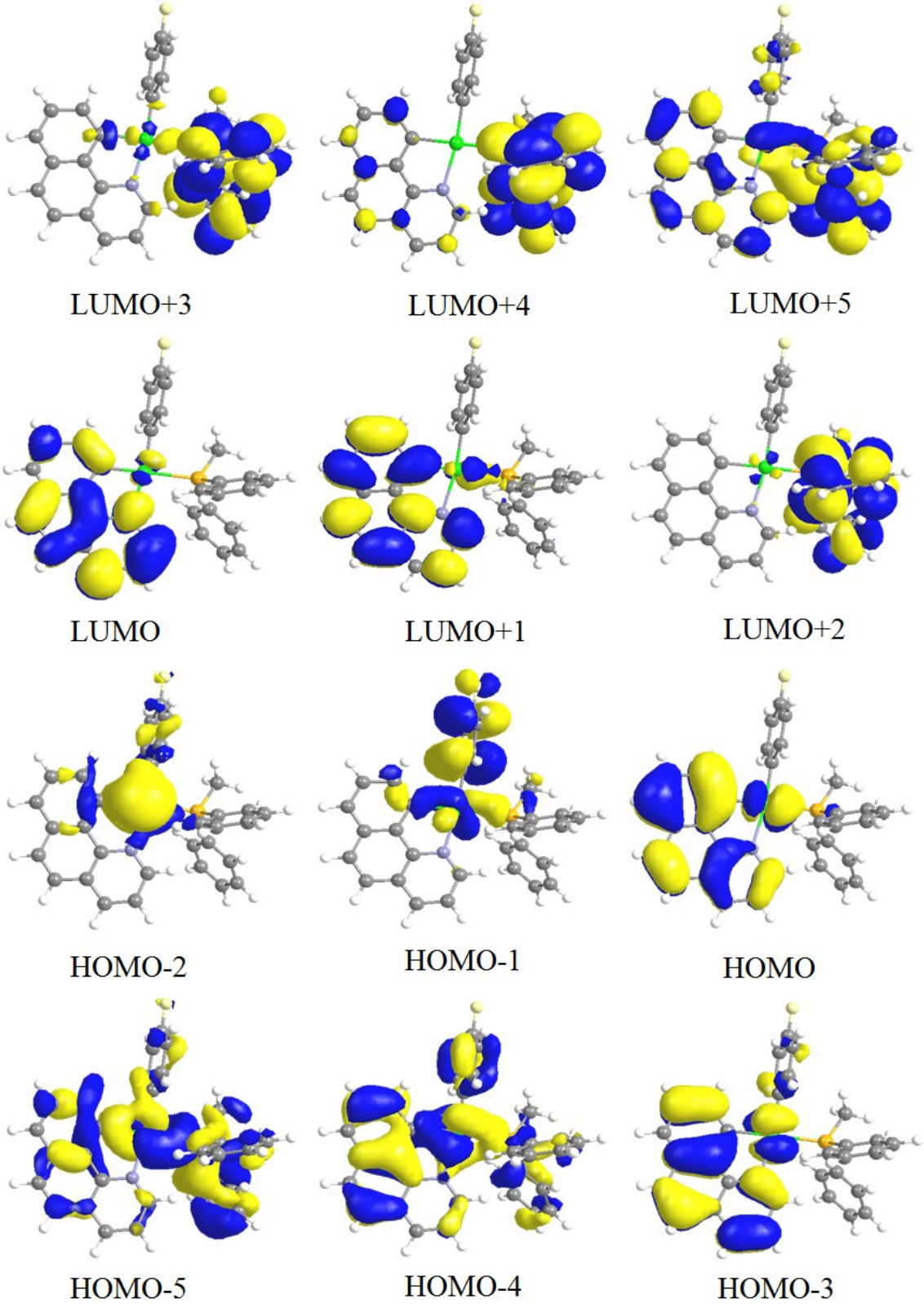

Figure S13. Qualitative frontier molecular orbitals for complex **2b.**

Table S18. Fragment contributions (%; from atomic orbital contributions) to the frontier orbitals of [Pt(*p*-F-C_6H_4)(bhq)(PPh_2Me)], **2b** in gas phase.

Energies(eV)	number	Pt	PPh_2Me	Bhq	*p*-F-C_6H_4
0.007	LUMO+6	4	13	78	5
-0.312	LUMO+5	1	94	4	1
-0.481	LUMO+4	6	88	5	1
-0.630	LUMO+3	6	87	6	1
-0.926	LUMO+2	2	93	4	1
-1.045	LUMO+1	4	14	81	1
-1.850	LUMO	2	1	96	1
-5.197	HOMO	20	3	77	0
-5.290	HOMO-1	23	5	9	63
-5.639	HOMO-2	82	2	9	7
-5.943	HOMO-3	49	1	45	5
-6.225	HOMO-4	36	2	4	58
-6.314	HOMO-5	49	2	24	25
-6.548	HOMO-6	15	42	41	2
-6.658	HOMO-7	39	4	56	1
-7.113	HOMO-8	7	82	5	6
-7.145	HOMO-9	14	54	14	18
-7.171	HOMO-10	7	76	7	10
-7.275	HOMO-11	34	42	12	12

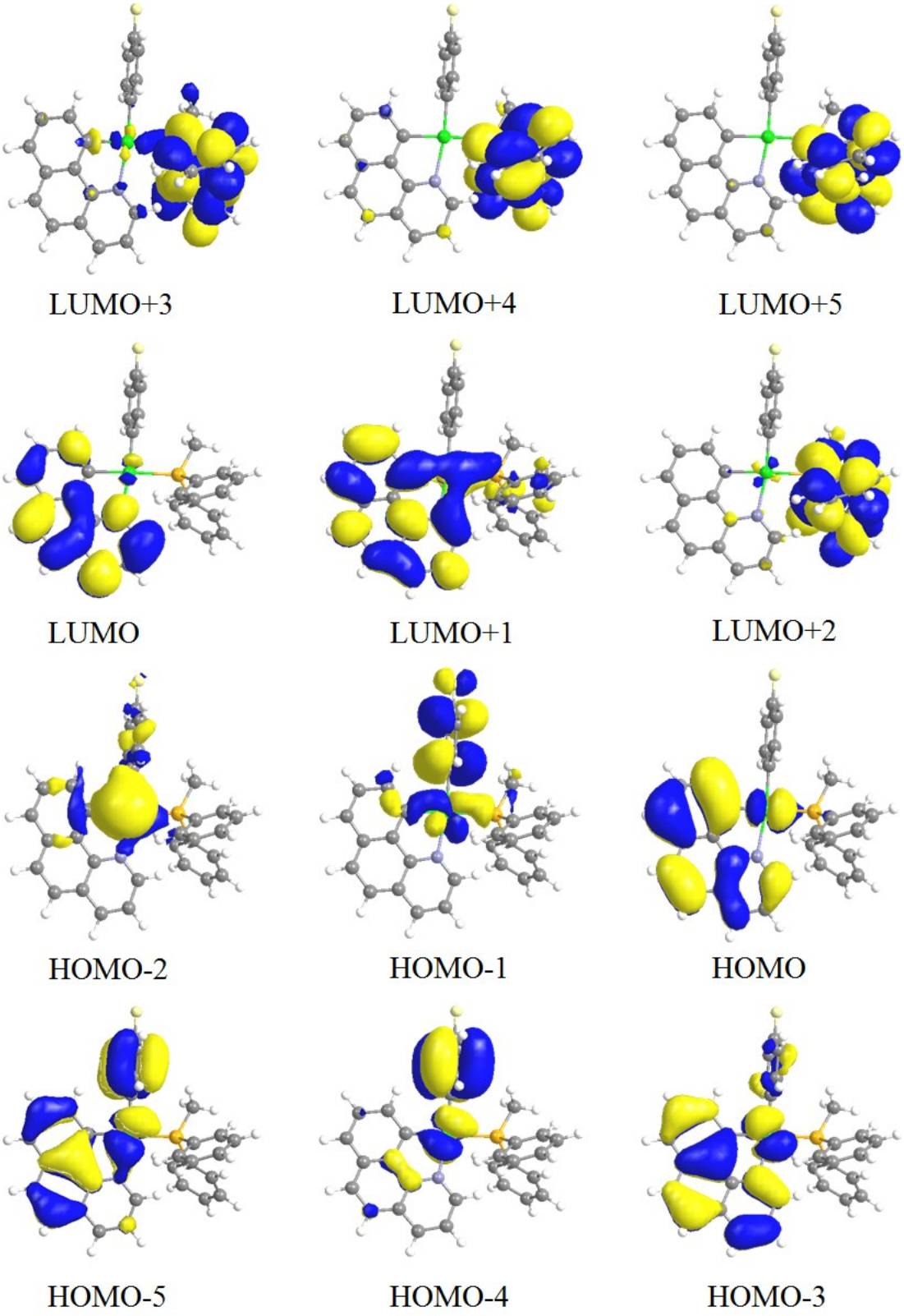

Figure S14. Qualitative frontier molecular orbitals for complex **2b** in gas phase.

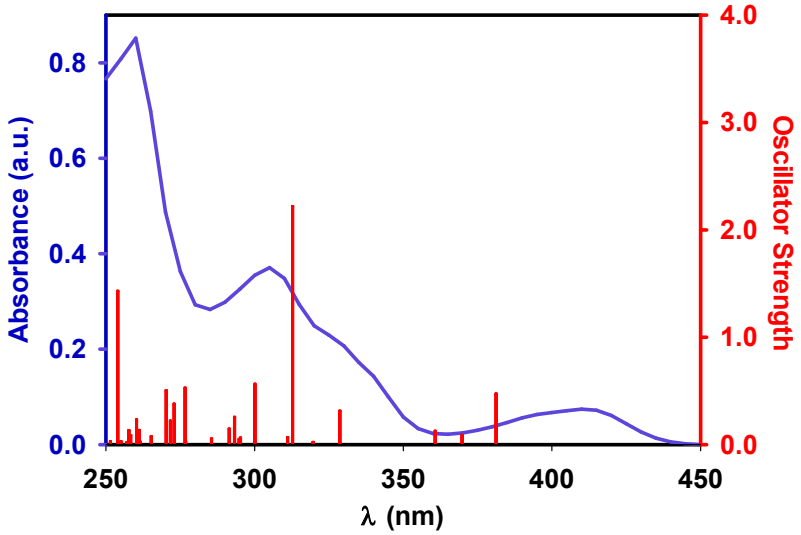

Figure S15. Experimental UV-vis spectra in CH_2Cl_2 (10^{-5} M) at 298 K and calculated absorption spectra, showing by bars, in CH_2Cl_2 for the complex **2b**.

Table S19. Selected vertical singlet excitations of **2b** from TDDFT calculations at the ground state geometry in CH_2Cl_2 solution (10^{-5}).

state	Monoexcitations[a]	Δ E/eV	λ_{cal}/nm	oscillator strength	main character
S1	H→L (93%)	3.257	381	0.047	MLCT/LC
S2	H-1→L (71%) H-2→L (27%)	3.357	369	0.0085	MLCT/LC/LLCT
S3	H-2→L (71%) H-1→L (27%)	3.441	360	0.0124	MLCT/LC/LLCT
S4	H-3→L (51%) H→L+1 (42%)	3.777	328	0.031	MLCT/LC
S6	H→L+1 (43%) H-3→L (31%) H-4→L (16%)	3.968	312	0.222	MLCT/LC/LLCT
S7	H-2→L+1 (88%)	3.990	311	0.0065	MLCT
S8	H-4→L (59%) H-3→L (12%) H-3→L+1 (11%)	4.135	300	0.056	MLCT/LC/LLCT
S11	H→L+2 (24%) H-3→L+1 (23%) H-7→L (17%) H-5→L (13%)	4.232	293	0.0252	MLCT/LC/LLCT
S12	H→L+2 (58%) H-3→L+1 (12%) H-7→L (10%)	4.258	291	0.0143	MLCT/LC/LLCT
S13	H-2→L+2 (91%)	4.346	285	0.0052	MLCT

Table S20. Lowest-energy vertical triplet excitations of **2b** from TDDFT calculations in gas phase.

state	Monoexcitations[a]	Δ E/eV	λ_{cal}/nm	main character
T1	H→L (71%) H-3→L (12%)	1.937	640	MLCT/LC
T2	H→L+1 (44%) H→L (24%) H-3→L (21%)	2.711	457	MLCT/LC/LLCT
T3	H-3→L (33%) H-1→L (32%) H→L+1 (26%)	2.841	436	MLCT/LC/LLCT
T4	H-1→L (52%) H-3→L (19%) H-2→L (17%)	2.900	427	MLCT/LC/LLCT
T5	H-2→L (78%) H-1→L (14%)	2.996	414	MLCT/LLCT

1.6. Complex 2c

Table S21. Fragment contributions (%; from atomic orbital contributions) to the frontier orbitals of [Pt(*p*-^{t}Bu-C_6H_4)(bhq)(PPh_2Me)], **2c** in CH_2Cl_2 solution.

Energies(eV)	number	Pt_1	PPh_2Me	Bhq	*p*-^{t}Bu-C_6H_4
-0.152	LUMO+6	4	46	46	4
-0.285	LUMO+5	6	65	27	2
-0.425	LUMO+4	5	86	8	1
-0.603	LUMO+3	9	82	7	1
-0.865	LUMO+2	3	94	2	1
-1.151	LUMO+1	4	6	89	1
-1.685	LUMO	3	2	94	1
-5.556	HOMO	25	5	10	60
-5.617	HOMO-1	28	3	67	2
-5.861	HOMO-2	82	2	7	9
-6.192	HOMO-3	45	1	45	9
-6.336	HOMO-4	16	3	4	77
-6.504	HOMO-5	44	9	40	7
-6.597	HOMO-6	22	40	35	3
-6.810	HOMO-7	50	7	42	1
-7.042	HOMO-8	1	96	2	1
-7.102	HOMO-9	2	95	2	1
-7.154	HOMO-10	5	78	7	10
-7.279	HOMO-11	18	36	22	24
-7.448	HOMO-12	20	30	30	20

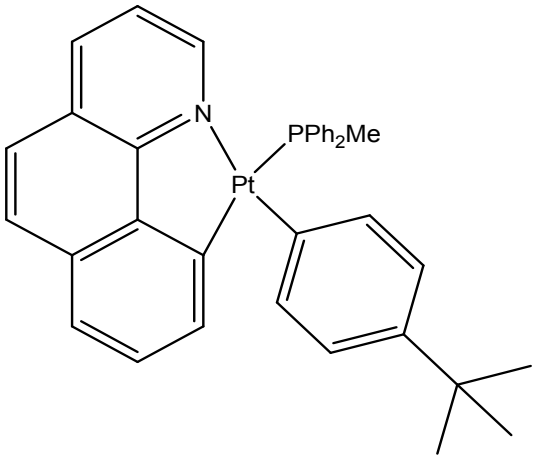

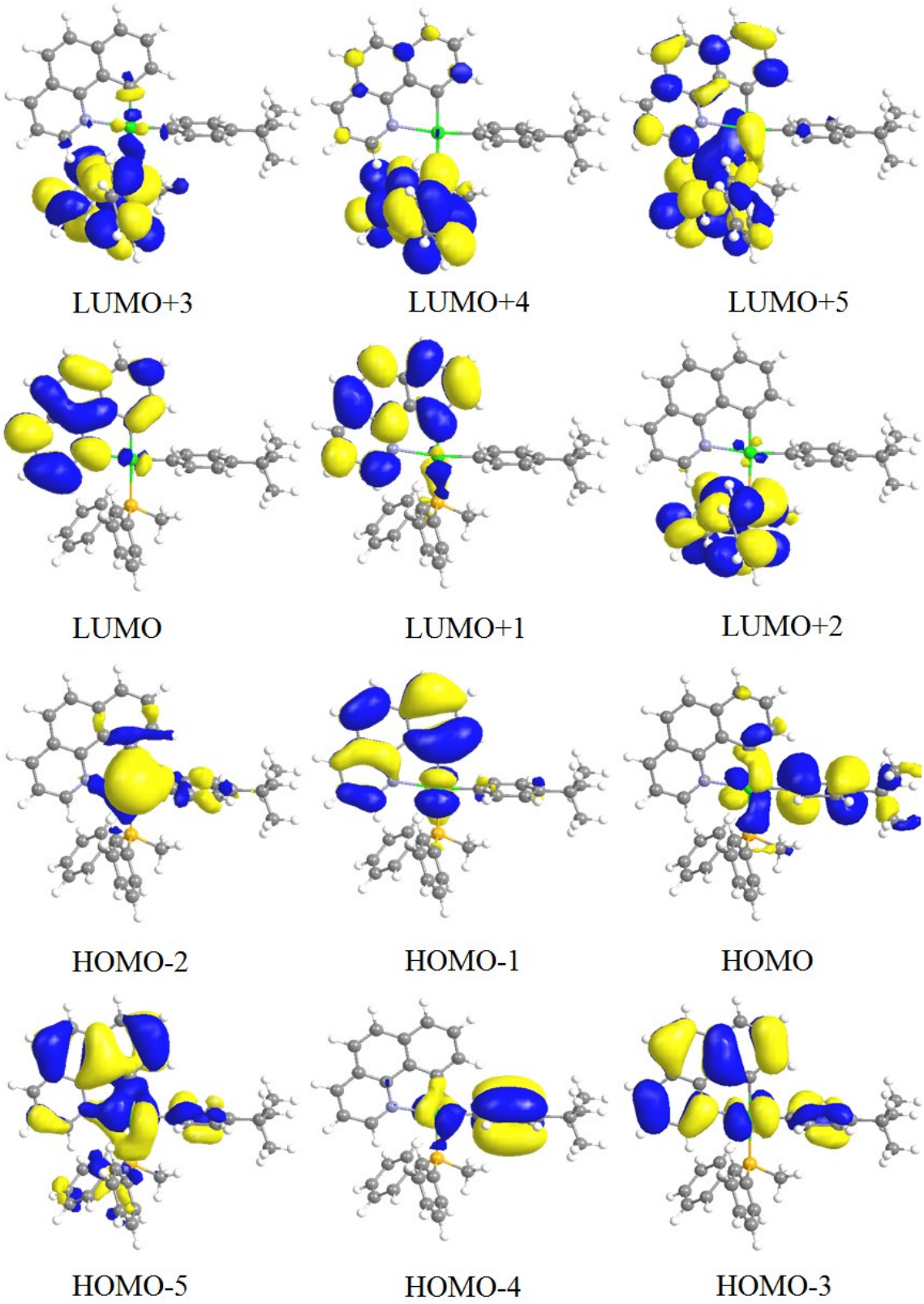

Figure S16. Qualitative frontier molecular orbitals for complex **2c.**

Table S22. Fragment contributions (%; from atomic orbital contributions) to the frontier orbitals of [Pt(*p*-^{t}Bu-C_6H_4)(bhq)(PPh_2Me)], **2c** in gas phase.

Energies(eV)	number	Pt_1	PPh_2Me	Bhq	*p*-^{t}Bu-C_6H_4
0.082	LUMO+6	4	12	80	4
-0.254	LUMO+5	2	94	4	0
-0.424	LUMO+4	6	89	4	1
-0.570	LUMO+3	5	88	6	1
-0.863	LUMO+2	2	93	4	1
-0.974	LUMO+1	4	13	81	2
-1.777	LUMO	2	1	96	1
-5.121	HOMO	20	3	77	0
-5.193	HOMO-1	24	5	8	63
-5.521	HOMO-2	80	2	9	9
-5.838	HOMO-3	42	1	35	22
-5.940	HOMO-4	25	2	11	62
-6.193	HOMO-5	64	1	28	7
-6.468	HOMO-6	16	41	41	2
-6.581	HOMO-7	39	4	57	0
-6.987	HOMO-8	20	15	23	43
-7.061	HOMO-9	1	93	3	3
-7.108	HOMO-10	1	96	2	1
-7.179	HOMO-11	51	16	12	21

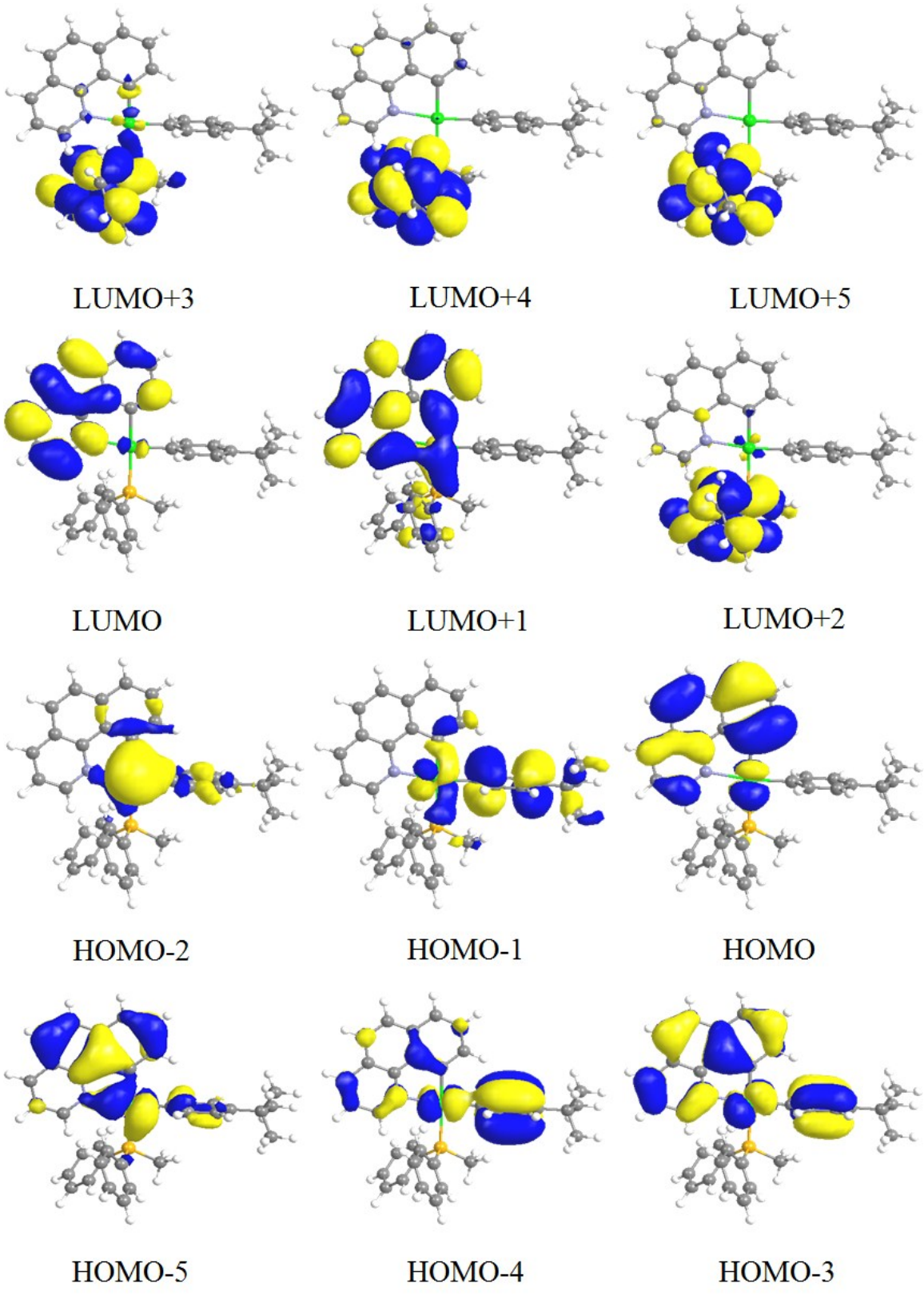

Figure S17. Qualitative frontier molecular orbitals for complex **2c** in gas phase**.**

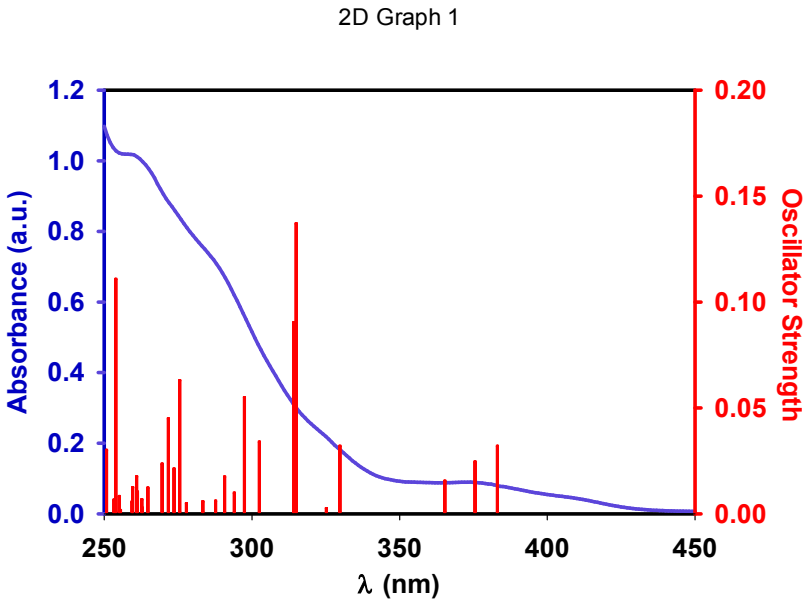

Figure S18. Experimental UV-vis spectra in CH_2Cl_2 (10^{-5} M) at 298 K and calculated absorption spectra, showing by bars, in CH_2Cl_2 for the complex **2c**.

Table S23. Selected vertical singlet excitations of **2c** from TDDFT calculations at the ground state geometry in CH_2Cl_2 solution (10^{-5}).

state	Monoexcitations[a]	Δ E/eV	λ_{cal}/nm	oscillator strength	main character
S1	H-1→L (65%) H→L (30%)	3.240	383	0.032	MLCT/LC/LLCT
S2	H→L (57%) H-1→L (25%) H-2→L (16%)	3.305	375	0.0244	MLCT/LC/LLCT
S3	H-2→L (82%) H→L (10%)	3.398	365	0.0153	MLCT/LC/LLCT
S4	H-3→L (46%) H-1→L+1 (33%) H→L+1 (12%)	3.764	329	0.032	MLCT/LC/LLCT
S6	H-2→L+1 (37%) H-1→L+1 (23%) H-3→L (20%)	3.940	315	0.137	MLCT/LC
S7	H-2→L+1 (55%) H-1→L+1 (19%) H-5→L (10%)	3.950	314	0.0903	MLCT/LC
S8	H-5→L (37%) H-4→L (32%) H-3→L (14%)	4.102	302	0.034	MLCT/LC/LLCT
S10	H-6→L (32%) H-3→L+1 (26%) H-4→L (21%)	4.172	297	0.055	MLCT/LC/LLCT
S11	H-6→L (56%) H-4→L (14%)	4.220	294	0.0097	MLCT/LC/LLCT
S13	H-3→L+1 (25%)	4.268	290	0.0173	MLCT/LC/LLCT

	H-7→L (21%) H-4→L (18%) H-5→L (17%)				
S14	H-2→L+2 (87%)	4.303	287	0.0059	MLCT
S17	H-5→L+1 (40%) H-7→L (19%) H-1→L+3 (10%)	4.503	275	0.063	MLCT/LC/LLCT

Table S24. Lowest-energy vertical triplet excitations of **2c** from TDDFT calculations in gas phase.

state	Monoexcitations[a]	Δ E/eV	λ_{cal}/nm	main character
T1	H→L (71%)	1.936	640	MLCT/LC
T2	H→L+1 (41%) H→L (25%) H-3→L (18%)	2.708	458	MLCT/LC/LLCT
T3	H-1→L (44%) H→L+1 (25%) H-3→L (18%)	2.826	439	MLCT/LC/LLCT
T4	H-1→L (34%) H-2→L (27%) H-3→L (19%) H→L+1 (10%)	2.885	430	MLCT/LC/LLCT
T5	H-2→L (68%) H-1→L (19%)	2.962	419	MLCT/LLCT

1.7. Complex 2d

Table S25. Fragment contributions (%; from atomic orbital contributions) to the frontier orbitals of [Pt(*p*-MeO-C_6H_4)(bhq)(PPh_2Me)], **2d** in CH_2Cl_2 solution.

Energies(eV)	number	Pt	PPh_2Me	Bhq	*p*-MeO-C_6H_4
-0.154	LUMO+6	4	49	44	3
-0.278	LUMO+5	6	62	29	3
-0.427	LUMO+4	5	86	8	1
-0.609	LUMO+3	10	81	7	2
-0.859	LUMO+2	3	94	2	1
-1.150	LUMO+1	4	6	89	1
-1.684	LUMO	3	2	94	1
-5.240	HOMO	18	4	6	72
-5.612	HOMO-1	30	3	67	0
-5.870	HOMO-2	83	2	8	7
-6.195	HOMO-3	47	1	47	5
-6.435	HOMO-4	27	5	10	58
-6.520	HOMO-5	28	14	35	23
-6.577	HOMO-6	25	37	36	2
-6.806	HOMO-7	49	7	42	2
-7.038	HOMO-8	3	93	2	2
-7.101	HOMO-9	4	92	3	1
-7.149	HOMO-10	13	67	8	12
-7.223	HOMO-11	45	25	8	22
-7.332	HOMO-12	15	45	26	14

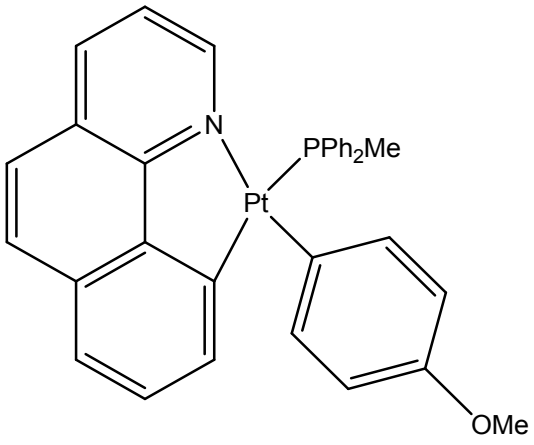

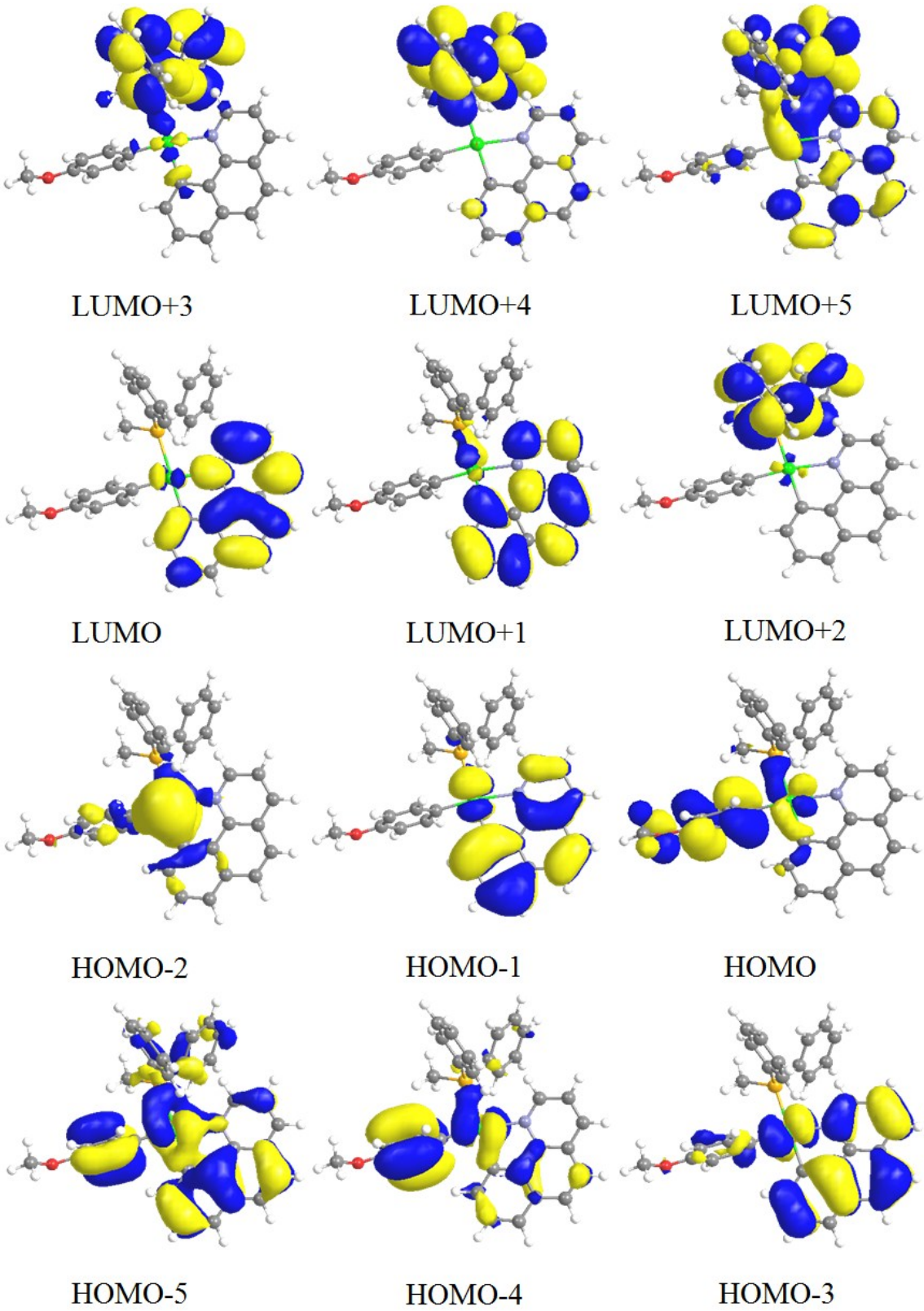

Figure S19. Qualitative frontier molecular orbitals for complex **2d.**

Table S26. Fragment contributions (%; from atomic orbital contributions) to the frontier orbitals of [Pt(*p*-MeO-C_6H_4)(bhq)(PPh_2Me)], **2d** in gas phase.

Energies(eV)	number	Pt	PPh_2Me	Bhq	*p*-MeO-C_6H_4
0.093	LUMO+6	4	12	80	4
-0.240	LUMO+5	3	93	4	0
-0.418	LUMO+4	5	89	5	1
-0.561	LUMO+3	6	87	6	1
-0.850	LUMO+2	3	92	4	1
-0.961	LUMO+1	4	15	80	1
-1.763	LUMO	2	1	96	1
-4.832	HOMO	16	4	6	74
-5.104	HOMO-1	21	2	77	0
-5.509	HOMO-2	81	2	10	7
-5.833	HOMO-3	51	1	41	7
-5.999	HOMO-4	17	2	2	79
-6.182	HOMO-5	61	2	28	9
-6.432	HOMO-6	14	42	42	2
-6.563	HOMO-7	39	4	57	0
-6.848	HOMO-8	52	6	12	30
-7.050	HOMO-9	1	96	2	1
-7.080	HOMO-10	17	41	17	25
-7.111	HOMO-11	6	77	7	10

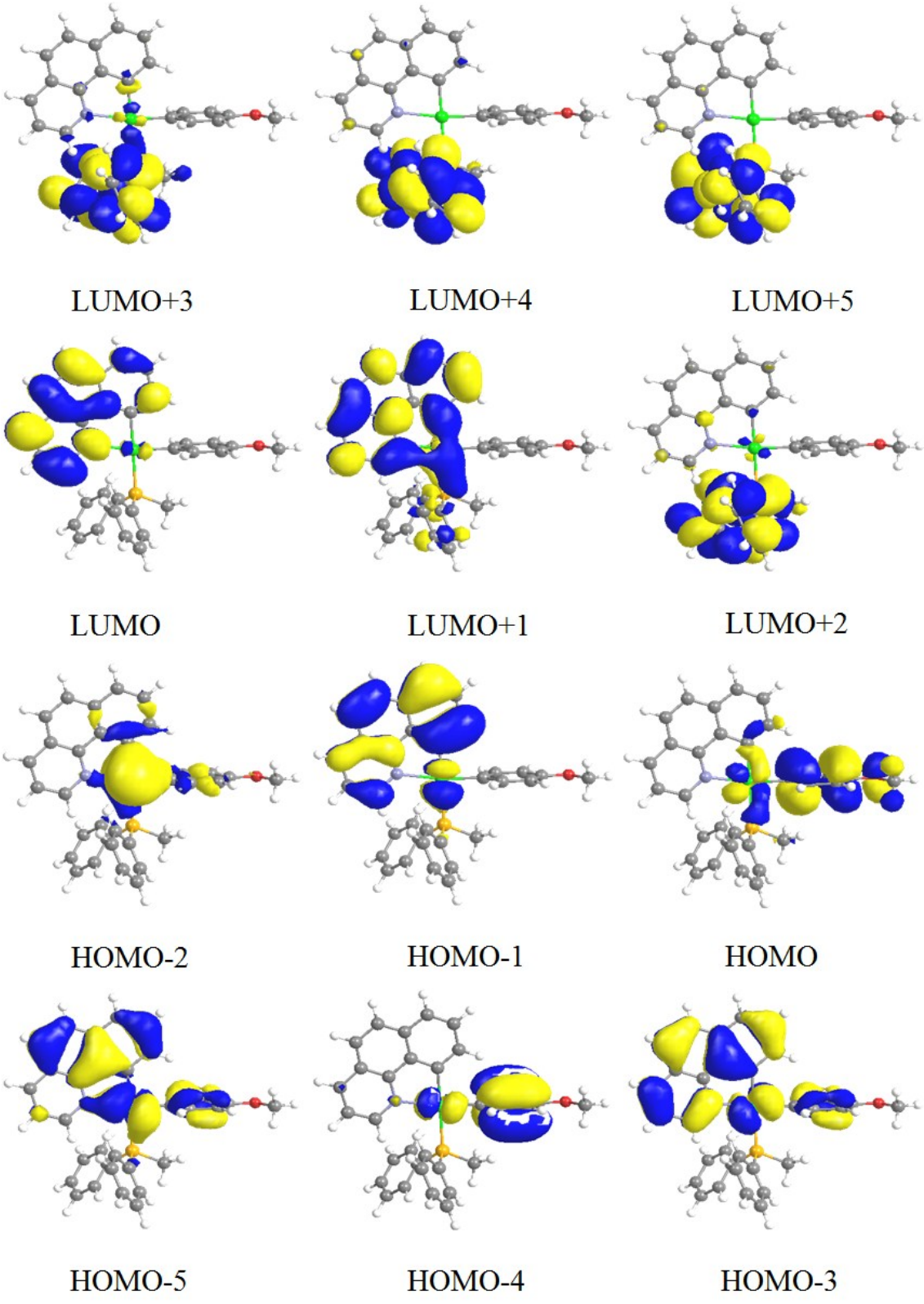

Figure S20. Qualitative frontier molecular orbitals for complex **2d** in gas phase**.**

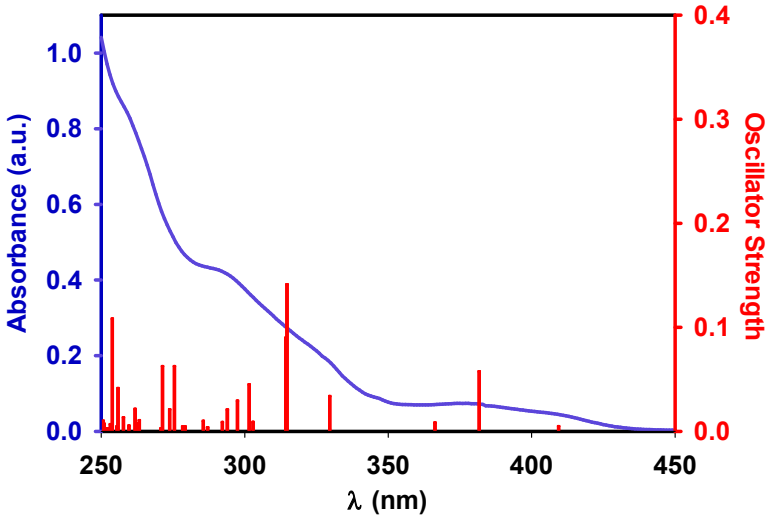

Figure S21. Experimental UV-vis spectra in CH_2Cl_2 (10^{-5} M) at 298 K and calculated absorption spectra, showing by bars, in CH_2Cl_2 for the complex **2d**.

Table S27. Selected vertical singlet excitations of **2d** from TDDFT calculations at the ground state geometry in CH_2Cl_2 solution (10^{-5}).

state	Monoexcitations[a]	Δ E/eV	λ_{cal}/nm	oscillator strength	main character
S1	H→L (97%)	3.033	409	0.0047	MLCT/LLCT
S2	H-1→L (92%)	3.252	381	0.0574	MLCT/LC
S3	H-2→L (97%)	3.389	366	0.0082	MLCT
S5	H-3→L (51%) H-1→L+1 (41%)	3.766	329	0.034	MLCT/LC
S7	H-2→L+1 (37%) H-1→L+1 (26%) H-3→L (21%)	3.944	314	0.1411	MLCT/LC
S8	H-2→L+1 (60%) H-1→L+1 (17%)	3.949	313	0.09	MLCT/LC
S9	H→L+3 (95%)	4.097	303	0.0088	MLCT/LLCT
S10	H-4→L (36%) H-5→L (32%) H-3→L (11%)	4.116	301	0.045	MLCT/LC/LLCT
S11	H-6→L (64%) H-3→L+1 (18%)	4.172	297	0.029	MLCT/LC/LLCT
S12	H-1→L+2 (23%) H-3→L+1 (23%) H-6→L (22%) H-7→L (18%)	4.222	294	0.021	MLCT/LC/LLCT
S13	H-1→L+2 (71%)	4.247			MLCT/LLCT
S16	H-5→L (47%) H-4→L (37%)	4.345	285	0.0098	MLCT/LC/LLCT
S17	H-5→L+1 (26%) H-7→L (21%) H-4→L+1 (17%)	4.444	275	0.0624	MLCT/LC/LLCT

	H-3→L+1 (11%)				

Table S28. Lowest-energy vertical triplet excitations of **2d** from TDDFT calculations in gas phase.

state	Monoexcitations[a]	Δ E/eV	λ_{cal}/nm	main character
T1	H-1→L (71%) H-3→L (11%)	1.936	641	MLCT/LC
T2	H→L (97%)	2.708	483	MLCT/LLCT
T3	H-1→L+1 (44%) H-1→L (24%) H-3→L (20%)	2.826	458	MLCT/LC/LLCT
T4	H-3→L (51%) H-1→L+1 (32%)	2.885	434	MLCT/LC/LLCT
T5	H-2→L (94%)	2.962	422	MLCT/LC/LLCT

1.8. Complex 3a

Table S29. Fragment contributions (%; from atomic orbital contributions) to the frontier orbitals of [Pt(bhq)(CF_3CO_2)(PPh_2Me)], **3a** in CH_2Cl_2 solution.

Energies(eV)	number	Pt	PPh_2Me	Bhq	CF_3CO_2
-0.337	LUMO+6	15	57	25	3
-0.443	LUMO+5	7	75	17	1
-0.523	LUMO+4	6	55	39	1
-0.884	LUMO+3	25	62	12	2
-0.987	LUMO+2	11	83	6	0
-1.342	LUMO+1	4	3	93	1
-1.933	LUMO	3	3	93	0
-5.814	HOMO	34	1	61	4
-6.417	HOMO-1	87	7	4	1
-6.498	HOMO-2	17	3	79	1
-6.936	HOMO-3	30	5	37	28
-6.976	HOMO-4	17	4	11	68
-7.076	HOMO-5	26	46	11	17
-7.097	HOMO-6	33	15	11	42
-7.115	HOMO-7	13	78	4	4
-7.170	HOMO-8	23	66	9	1
-7.211	HOMO-9	11	82	5	2
-7.300	HOMO-10	41	51	8	1
-7.645	HOMO-11	8	5	34	53

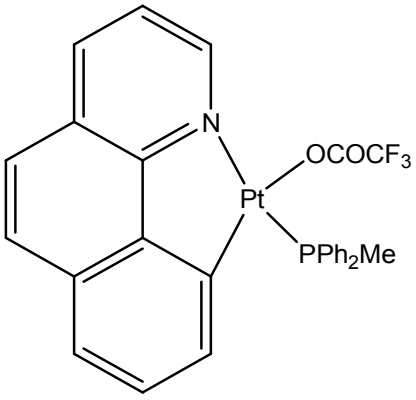

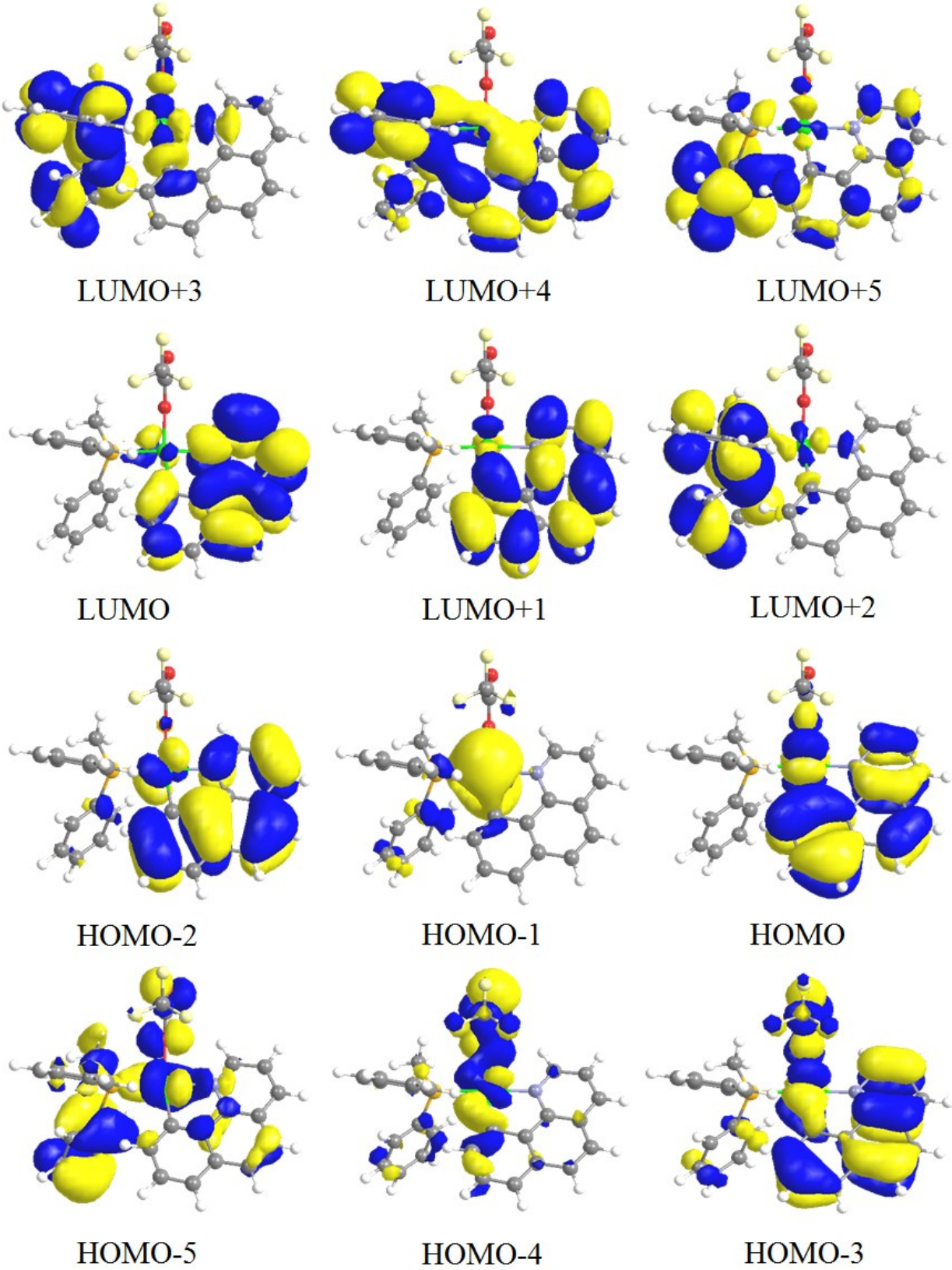

Figure S22. Qualitative frontier molecular orbitals for complex **3a.**

Table S30. Fragment contributions (%; from atomic orbital contributions) to the frontier orbitals of [Pt(bhq)(CF_3CO_2)(PPh_2Me)], **3a** in gas phase.

Energies(eV)	number	Pt	PPh_2Me	Bhq	CF_3CO_2
-0.235	LUMO+6	13	31	53	3
-0.416	LUMO+5	4	81	14	1
-0.540	LUMO+4	5	87	8	0
-0.843	LUMO+3	20	70	9	1
-1.009	LUMO+2	6	91	3	0
-1.331	LUMO+1	3	2	94	1
-2.025	LUMO	5	4	91	1
-5.472	HOMO	33	1	60	6
-6.378	HOMO-1	11	2	12	76
-6.419	HOMO-2	27	2	58	13
-6.439	HOMO-3	75	7	16	2
-6.583	HOMO-4	25	2	14	58
-6.762	HOMO-5	29	4	27	40
-7.100	HOMO-6	48	34	15	3
-7.122	HOMO-7	18	68	14	1
-7.190	HOMO-8	9	83	7	1
-7.252	HOMO-9	3	95	0	2
-7.317	HOMO-10	15	78	5	2
-7.430	HOMO-11	23	4	40	33

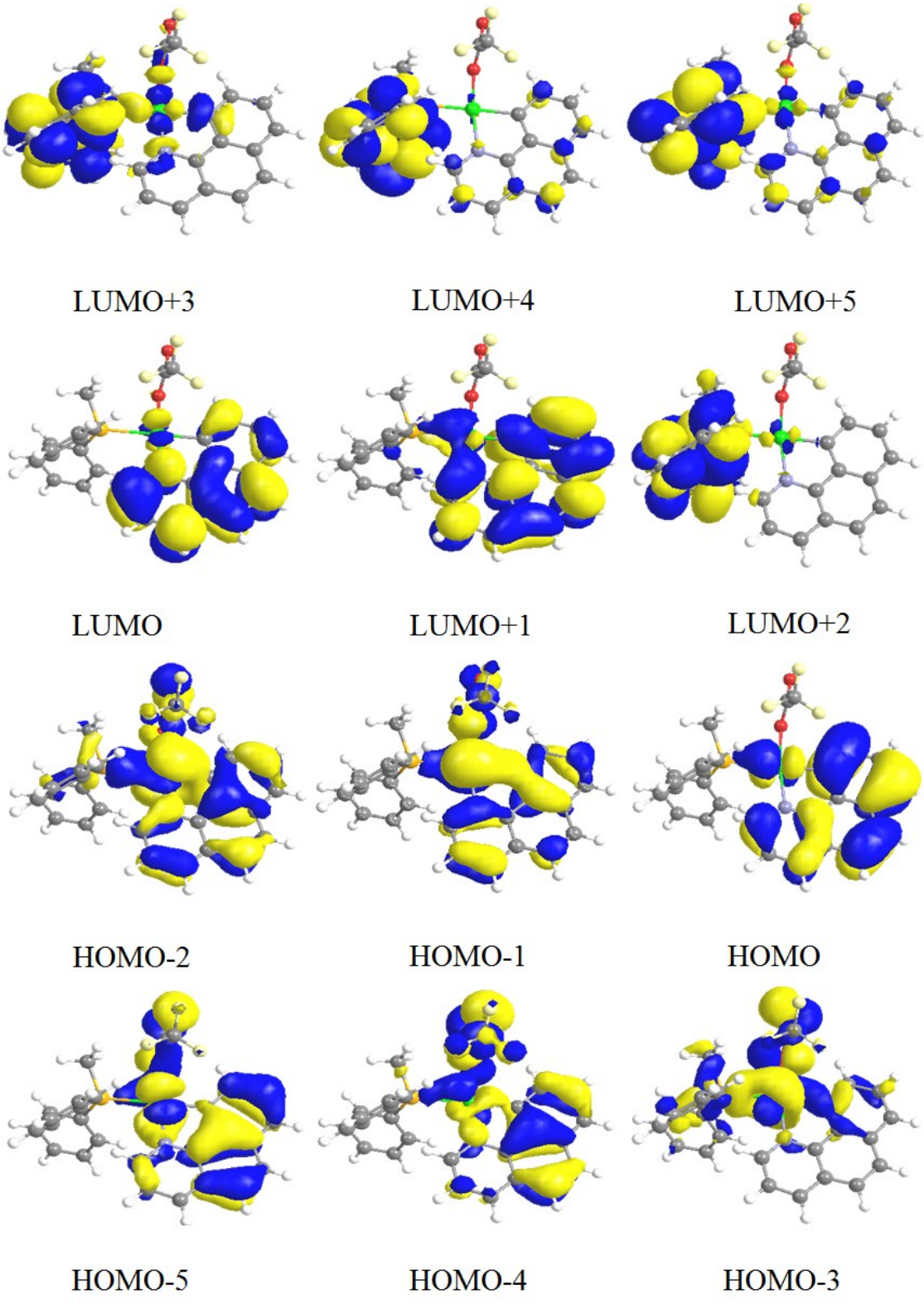

Figure S23. Qualitative frontier molecular orbitals for complex **3a** in gas phase**.**

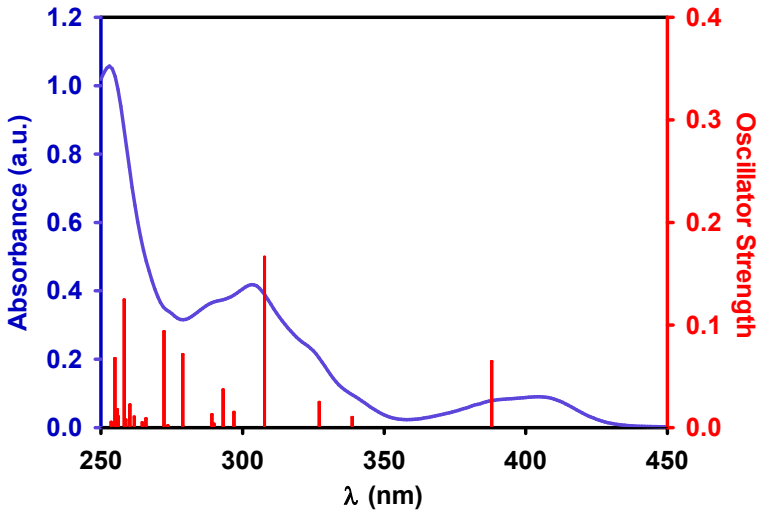

Figure S24. Experimental UV-vis spectra in CH_2Cl_2 (10^{-5} M) at 298 K and calculated absorption spectra, showing by bars, in CH_2Cl_2 for the complex **3a**.

Table S31. Selected vertical singlet excitations of **3a** from TDDFT calculations at the ground state geometry in CH_2Cl_2 solution (10^{-5}).

state	Monoexcitations[a]	ΔE/eV	λ_{cal}/nm	oscillator strength	main character
S1	H→L (96%)	3.200	387	0.064	MLCT/LC
S2	H-1→L (97%)	3.665	338	0.0099	MLCT
S3	H→L+1 (56%) H-2→L (39%)	3.795	327	0.0245	MLCT/LC/LLCT
S4	H→L+3 (56%) H→L+2 (18%)	3.941	315	0.0011	MLCT/LC/LLCT
S5	H-2→L (53%) H→L+1 (37%)	4.033	307	0.166	MLCT/LC/LLCT
S6	H-1→L+3 (49%) H-1→L+6 (13%) H-1→L+2 (11%)	4.179	297	0.0148	MLCT
S7	H-3→L (35%) H-2→L+1 (31%)	4.234	293	0.0368	MLCT/LC/LLCT
S9	H-1→L+1 (91%)	4.291	289	0.0126	MLCT
S11	H-5→L (19%) H-10→L (16%) H-3→L (14%) H-8→L (12%) H-7→L (12%)	4.449	279	0.0712	MLCT/LC/LLCT
S13	H→L+4 (25%) H-3→L (21%) H-5→L (20%) H-2→L+1 (10%)	4.557	272	0.0935	MLCT/LC/LLCT
S14	H-5→L (16%) H→L+6 (13%) H-6→L (11%)	4.667	266	0.0086	MLCT/LC/LLCT

	H→L+3 (11%)				
S19	H→L+4 (31%) H-8→L (15%) H→L+6 (10%) H-2→L+1 (10%)	4.805	258	0.1244	MLCT/LC/LLCT
S22	H→L+5 (15%) H-6→L+3 (12%)	4.866	255	0.0673	MLCT/LC/LLCT

Table S32. Lowest-energy vertical triplet excitations of **3a** from TDDFT calculations in gas phase.

state	Monoexcitations[a]	Δ E/eV	λ_{cal}/nm	main character
T1	H→L (67%) H→L+1 (20%)	2.259	549	MLCT/LC
T2	H→L+1 (42%) H→L (30%) H-2→L (11%)	2.593	478	MLCT/LC/LLCT
T3	H-2→L (49%) H→L+1 (26%) H-3→L (10%)	2.995	414	MLCT/LC/LLCT
T4	H-3→L (76%) H-2→L (10%)	3.422	362	MLCT/LC/LLCT
T5	H→L+3 (29%) H-4→L (18%) H-5→L (13%) H→L+7 (11%)	3.563	348	MLCT/LC/LLCT

1.9. Complex 3b

Table S33. Fragment contributions (%; from atomic orbital contributions) to the frontier orbitals of [Pt(bhq)(Cl)(PPh_2Me)], **3b** in CH_2Cl_2 solution.

Energies(eV)	number	Pt	PPh_2Me	Bhq	Cl
-0.339	LUMO+6	12	55	30	3
-0.430	LUMO+5	11	73	12	4
-0.511	LUMO+4	7	63	30	1
-0.909	LUMO+3	28	52	16	4
-0.951	LUMO+2	7	89	4	0
-1.288	LUMO+1	4	3	92	1
-1.871	LUMO	3	4	93	0
-5.700	HOMO	36	1	52	11
-6.358	HOMO-1	85	7	7	1
-6.441	HOMO-2	21	3	73	3
-6.689	HOMO-3	29	3	6	61
-6.746	HOMO-4	23	1	45	31
-7.027	HOMO-5	35	53	11	1
-7.086	HOMO-6	11	83	4	1
-7.125	HOMO-7	29	57	12	1
-7.177	HOMO-8	7	90	3	0
-7.263	HOMO-9	22	64	10	5
-7.425	HOMO-10	9	6	42	43
-7.522	HOMO-11	17	4	37	43

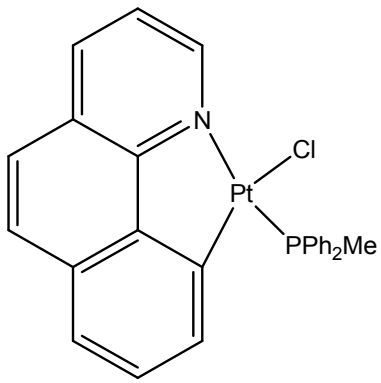

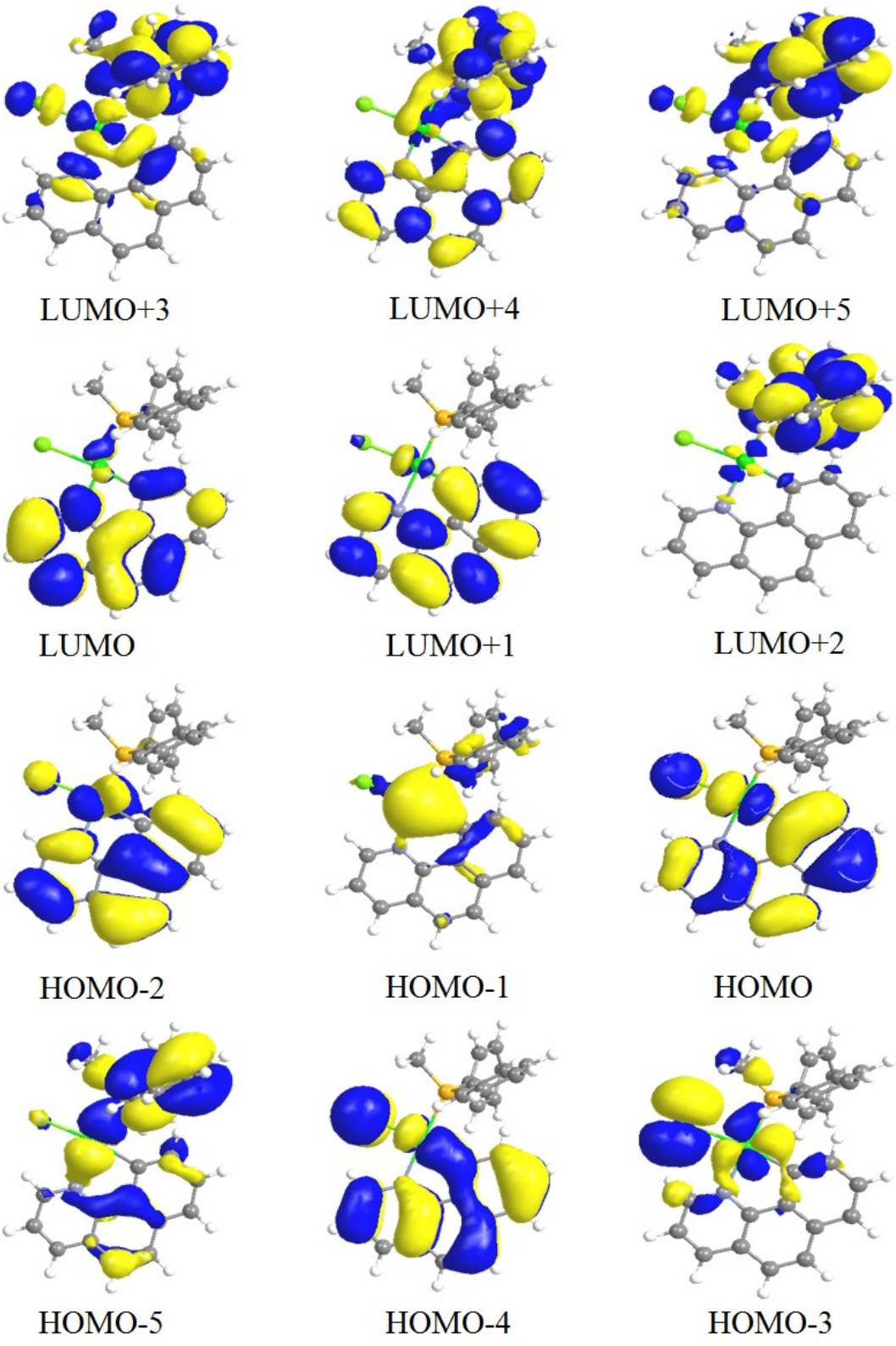

Figure S25. Qualitative frontier molecular orbitals for complex **3b.**

Table S34. Fragment contributions (%; from atomic orbital contributions) to the frontier orbitals of [Pt(bhq)(Cl)(PPh_2Me)], **3b** in gas phase.

Energies(eV)	number	Pt	PPh_2Me	Bhq	Cl
-0.108	LUMO+6	7	22	70	1
-0.302	LUMO+5	7	85	6	2
-0.433	LUMO+4	6	81	12	0
-0.698	LUMO+3	21	66	11	2
-0.885	LUMO+2	2	95	3	0
-1.182	LUMO+1	6	6	87	1
-1.967	LUMO	2	2	96	0
-5.236	HOMO	32	1	49	18
-5.975	HOMO-1	22	2	49	26
-6.030	HOMO-2	23	3	7	67
-6.143	HOMO-3	86	5	8	1
-6.424	HOMO-4	14	1	55	30
-6.853	HOMO-5	27	7	35	30
-6.873	HOMO-6	43	10	31	16
-6.964	HOMO-7	7	75	16	3
-7.041	HOMO-8	3	89	7	2
-7.125	HOMO-9	14	62	15	10
-7.130	HOMO-10	13	56	19	11
-7.228	HOMO-11	16	73	7	4

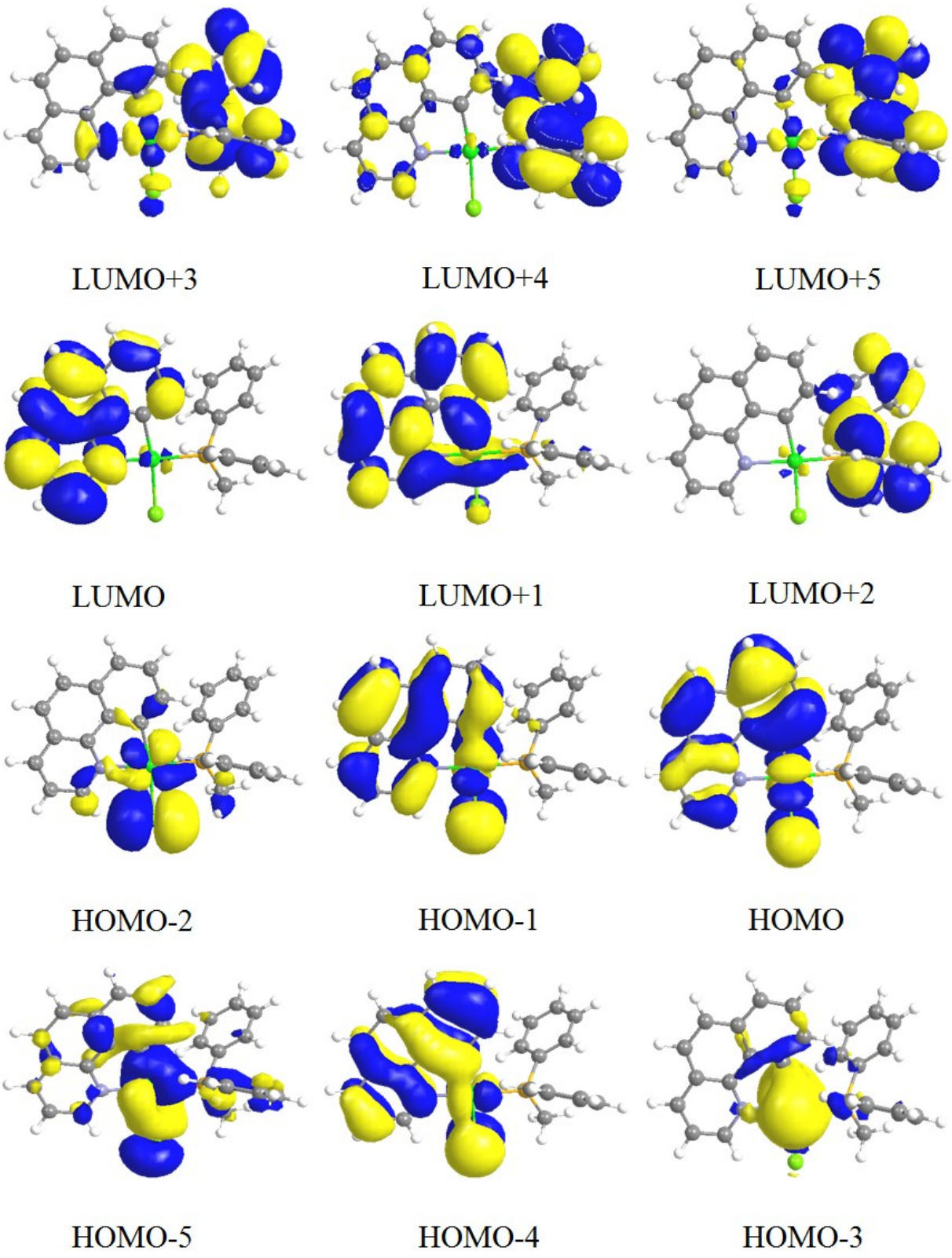

Figure S26. Qualitative frontier molecular orbitals for complex **3b** in gas phase**.**

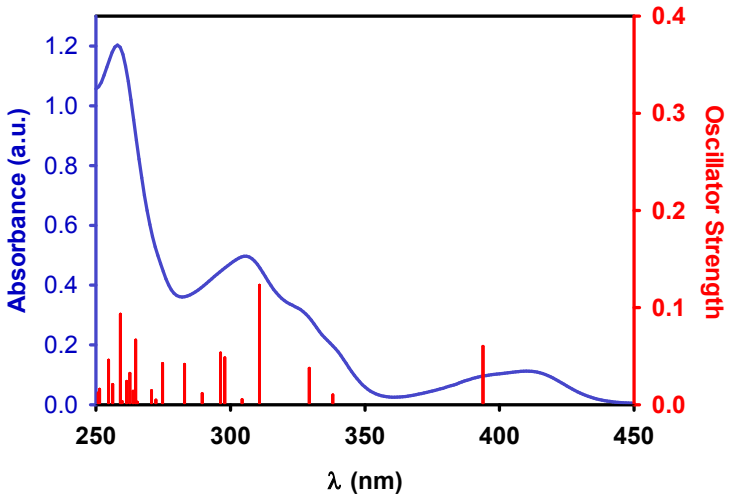

Figure S27. Experimental UV-vis spectra in CH_2Cl_2 (10^{-5} M) at 298 K and calculated absorption spectra, showing by bars, in CH_2Cl_2 for the complex **3b**.

Table S35. Selected vertical singlet excitations of **3b** from TDDFT calculations at the ground state geometry in CH_2Cl_2 solution (10^{-5}).

state	Monoexcitations[a]	Δ E/eV	λ_{cal}/nm	oscillator strength	main character
S1	H→L (96%)	3.148	394	0.0602	MLCT/LC/LLCT
S2	H-1→L (93%)	3.668	338	0.0102	MLCT
S3	H→L+3 (70%)	3.759	330	0.0016	MLCT/LC/LLCT
S4	H-2→L (25%) H→L+1 (66%)	3.766	329	0.0377	MLCT/LC
S5	H-2→L (22%) H→L+1 (61%)	3.990	311	0.1231	MLCT/LC
S8	H-1→L+2 (22%) H-2→L+2 (16%)	4.163	298	0.0484	MLCT/LLCT
S9	H→L+2 (44%) H-4→L (33%) H-2→L+1 (10%)	4.185	296	0.0533	MLCT/LC/LLCT
S10	H-1→L+1 (94%)	4.284	289	0.0116	MLCT
S11	H-2→L+1 (26%) H-5→L (22%) H-4→L (15%) H-7→L (10%)	4.383	283	0.0417	MLCT/LC/LLCT
S12	H→L+4 (33%) H-5→L (26%) H→L+6 (10%)	4.513	275	0.0426	MLCT/LC/LLCT

Table S36. Lowest-energy vertical triplet excitations of **3b** from TDDFT calculations in gas phase.

state	Monoexcitations[a]	Δ E/eV	λ_{cal}/nm	main character

T1	H→L (60%) H-1→L (23%)	1.973	628	MLCT/LC/LLCT
T2	H→L+1 (36%) H→L (35%), H-1→L (16%)	2.617	474	MLCT/LC/LLCT
T3	H→L+1 (40%) H-1→L (37%)	2.842	436	MLCT/LC/LLCT
T4	H-3→L (82%)	3.331	372	MLCT
T5	H-2→L (93%)	3.360	369	MLCT/LLCT

1.10. Complex 3c

Table S37. Fragment contributions (%; from atomic orbital contributions) to the frontier orbitals of [Pt(bhq)(I)(PPh_2Me)], **3c** in CH_2Cl_2 solution.

Energies(eV)	number	Pt	PPh_2Me	Bhq	I
-0.346	LUMO+6	6	54	39	1
-0.472	LUMO+5	15	72	9	5
-0.580	LUMO+4	5	68	25	2
-0.921	LUMO+3	4	93	3	0
-1.163	LUMO+2	30	38	25	7
-1.343	LUMO+1	10	8	81	2
-1.904	LUMO	3	4	93	0
-5.680	HOMO	34	1	43	22
-6.126	HOMO-1	14	3	6	77
-6.231	HOMO-2	44	4	26	25
-6.434	HOMO-3	46	5	30	20
-6.518	HOMO-4	11	3	67	19
-6.791	HOMO-5	26	4	36	33
-7.030	HOMO-6	37	51	12	1
-7.088	HOMO-7	27	63	9	0
-7.097	HOMO-8	15	75	10	0
-7.180	HOMO-9	3	94	3	0
-7.206	HOMO-10	27	35	29	9
-7.390	HOMO-11	41	38	16	5
-7.882	HOMO-12	75	9	13	4

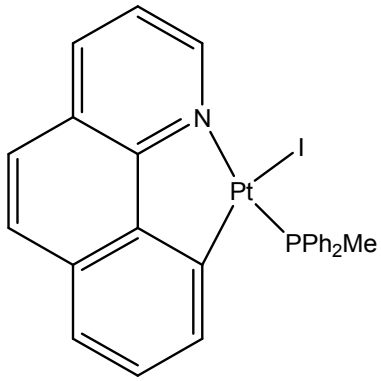

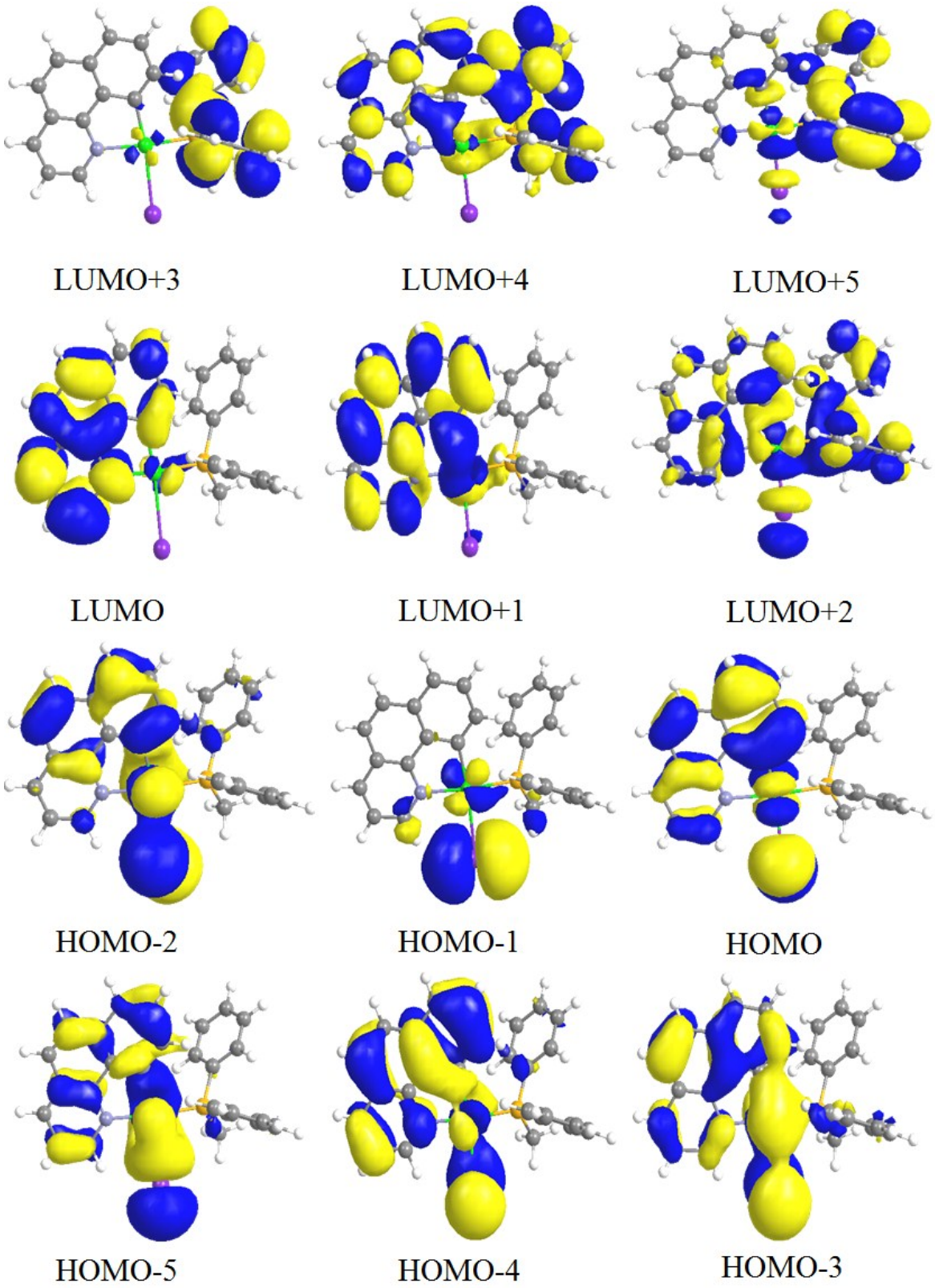

Figure S28. Qualitative frontier molecular orbitals for complex **3c.**

Table S38. Fragment contributions (%; from atomic orbital contributions) to the frontier orbitals of [Pt(bhq)(I)(PPh_2Me)], **3c** in gas phase.

Energies(eV)	number	Pt	PPh_2Me	Bhq	I
-0.245	LUMO+6	8	56	34	2
-0.351	LUMO+5	9	79	7	4
-0.501	LUMO+4	6	77	15	1
-0.839	LUMO+3	28	52	17	4
-0.900	LUMO+2	2	95	2	1
-1.263	LUMO+1	7	5	87	1
-2.040	LUMO	2	2	96	0
-5.155	HOMO	27	1	27	45
-5.462	HOMO-1	11	3	7	78
-5.741	HOMO-2	5	2	63	29
-6.096	HOMO-3	40	4	31	24
-6.266	HOMO-4	45	2	47	6
-6.463	HOMO-5	45	5	32	18
-6.923	HOMO-6	59	17	24	0
-6.993	HOMO-7	29	44	25	2
-7.035	HOMO-8	20	54	24	2
-7.088	HOMO-9	9	85	5	1
-7.142	HOMO-10	3	96	2	0
-7.246	HOMO-11	19	76	5	1

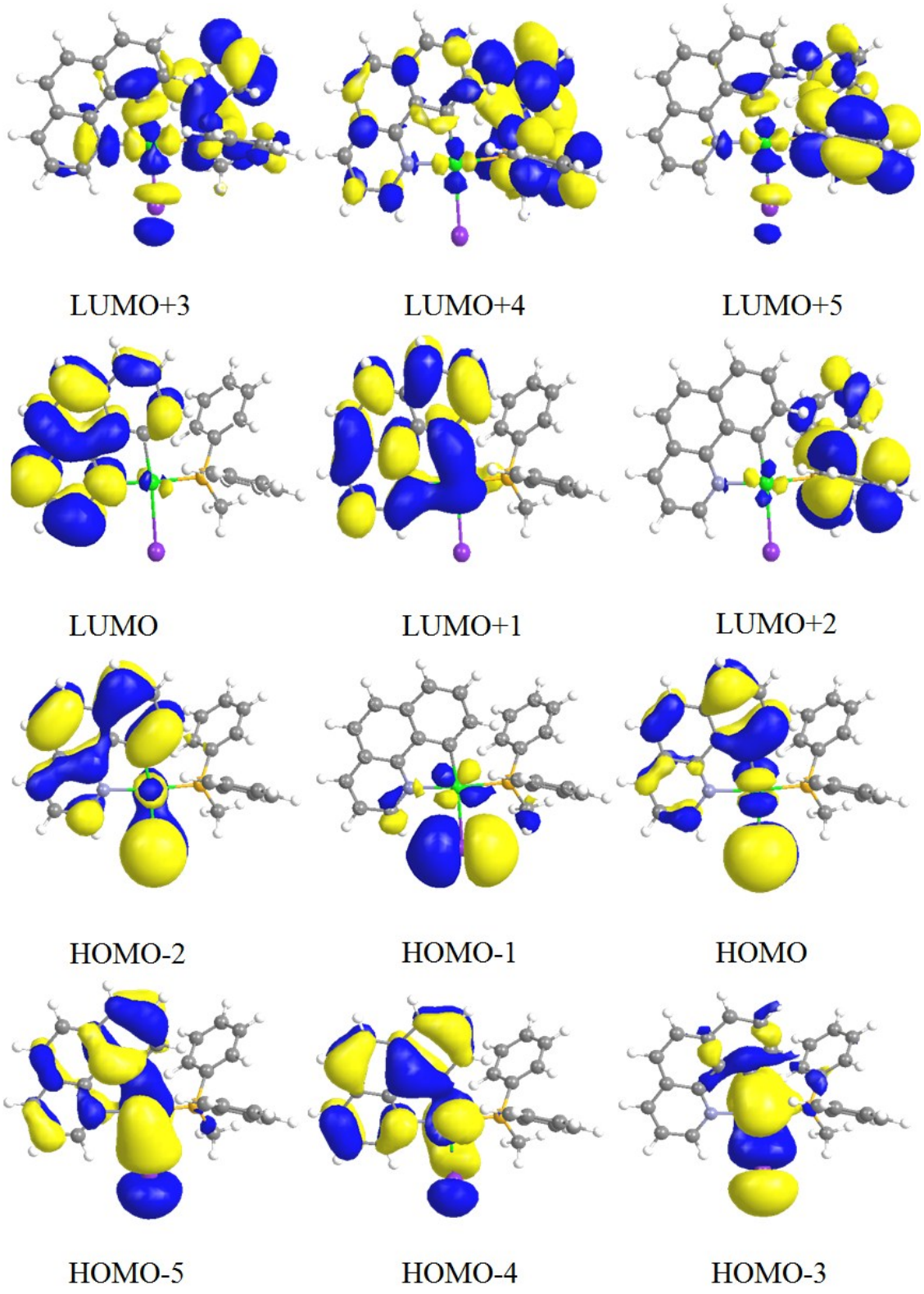

Figure S29. Qualitative frontier molecular orbitals for complex **3c** in gas phase**.**

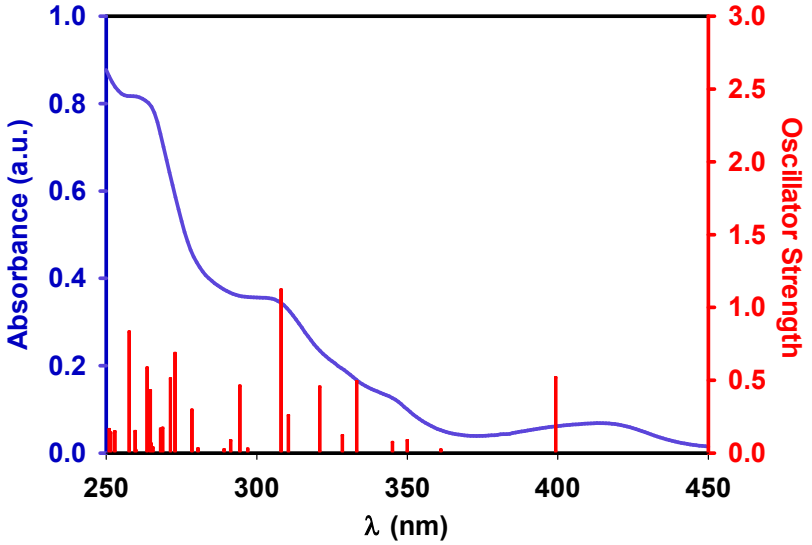

Figure S30. Experimental UV-vis spectra in CH_2Cl_2 (10^{-5} M) at 298 K and calculated absorption spectra, showing by bars, in CH_2Cl_2 for the complex **3c**.

Table S39. Selected vertical singlet excitations of **3c** from TDDFT calculations at the ground state geometry in CH_2Cl_2 solution (10^{-5}).

state	Monoexcitations[a]	Δ E/eV	λ_{cal}/nm	oscillator strength	main character
S1	H→L (96%)	3.109	399	0.0517	MLCT/LC/LLCT
S2	H→L+2 (65%) H→L+1 (19%)	3.437	361	0.0021	MLCT/LC/LLCT
S3	H-2→L (47%) H-1→L (31%)	3.547	350	0.0085	MLCT/LC/LLCT
S5	H→L+1 (27%) H-2→L+2 (18%)	3.726	333	0.0491	MLCT/LC/LLCT
S6	H→L+1 (32%) H-2→L+2 (17%) H→L+2 (13%) H-3→L+2 (10%)	3.779	328	0.0119	MLCT/LC/LLCT
S7	H-3→L (76%) H-2→L (10%)	3.868	320	0.0453	MLCT/LC/LLCT
S8	H-1→L+2 (54%) H-1→L+1 (23%)	3.997	310	0.0256	MLCT/LLCT
S10	H-4→L (71%)	4.028	308	0.112	MLCT/LC/LLCT
S12	H-2→L+1 (28%) H-1→L+1 (18%) H-5→L (13%) H-3→L+1 (11%)	4.216	294	0.0459	MLCT/LC/LLCT
S13	H-1→L+1 (48%) H-1→L+2 (19%) H-2→L+1 (18%)	4.260	291	0.0084	MLCT/LC/LLCT
S18	H→L+5 (32%) H→L+4 (15%)	4.548	273	0.0684	MLCT/LC/LLCT

	H-6→ (14%)				
S19	H-3→L+1 (24%) H-4→L+1 (22%) H-3→L+2 (14%) H-4→L+2 (13%)	4.573	280	0.0509	MLCT/LC/LLCT
S28	H→L+6 (33%) H-5→L+1 (31%)	4.816	257	0.0831	MLCT/LC/LLCT

Table S40. Lowest-energy vertical triplet excitations of **3c** from TDDFT calculations in gas phase.

state	Monoexcitations[a]	Δ E/eV	λ_{cal}/nm	main character
T1	H→L (44%) H-2→L (32%)	1.981	626	MLCT/LC/LLCT
T2	H→L (48%) H→L+1 (19%) H-4→L (10%)	2.534	489	MLCT/LC/LLCT
T3	H-1→L (96%)	2.789	444	MLCT/LLCT
T4	H→L+1 (39%) H-2→L (22%) H-2→L+1 (13%)	2.809	441	MLCT/LLCT
T5	H-4→L (49%) H-2→L (31%)	3.055	406	MLCT/LC/LLCT

1.11. Emission spectra in dichloromethane

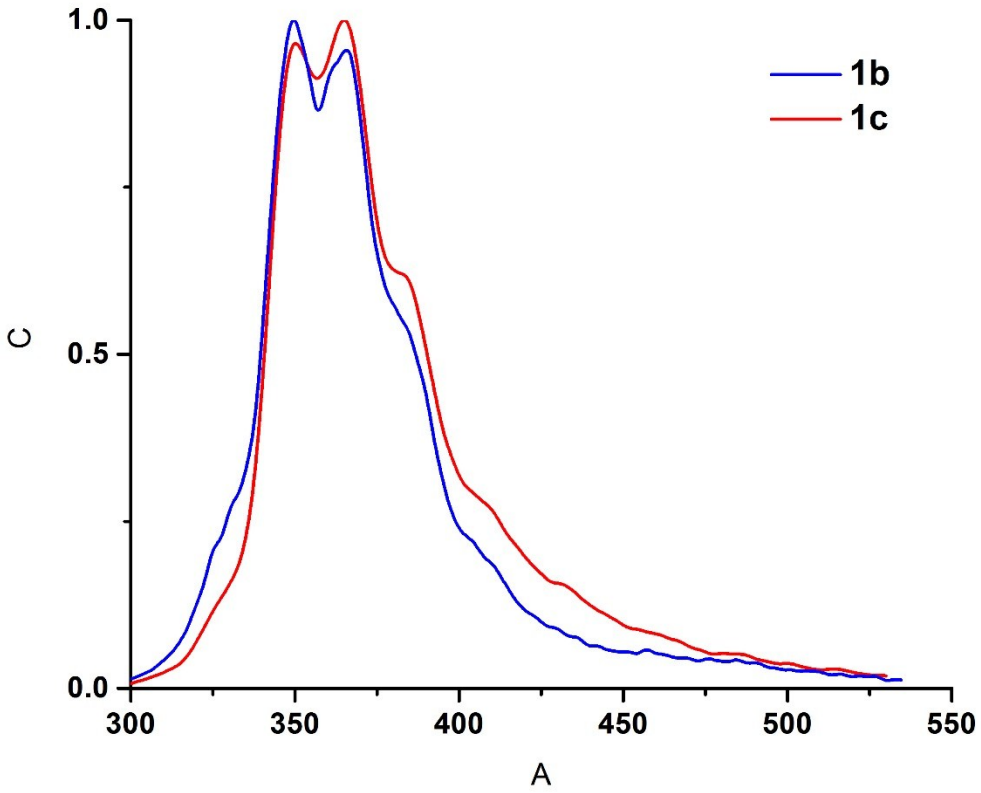

Figure S31. Experimental emission spectra of **1b** and **1c** in CH_2Cl_2 (10^{-5} M) at 298 K.

2. Supplementary computational data

Table S41. Selected bond distances (Å) and angles (deg) of the optimized structures of Complexes **1** in the ground state.

	1a(calc.)	**1b**(calc.)	**1b**(exp.)	**1c**(calc.)	**1c**(exp.)
Pt–N	2.237	2.222	2.145	2.218	2.145
Pt–P	2.422	2.404	2.294	2.393	2.294
Pt–C(1)	2.024	2.027	2.013	2.026	2.013
Pt–C(2)	2.045	2.047	2.041	2.047	2.041
C(1)-Pt-C(2)	91.3	92.2	90.5	92.3	90.5
C(1)-Pt-N	170.5	171.7	170.9	171.9	170.9
C(1)-Pt-P	91.4	88.2	90.4	89.3	90.4
P-Pt-C(2)	176.9	179.4	176.4	177.1	176.4
P-Pt-N	98.0	100.0	98.6	98.7	98.6
C(2)-Pt-N	79.4	79.5	80.4	79.6	80.4

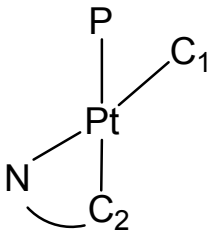

Table S42. Selected bond distances (Å) and angles (deg) of the optimized structures of Complexes **2** in the ground state.

	2a(calc.)	**2b**(calc.)	**2c**(calc.)	**2d**(calc.)
Pt–N	2.221	2.217	2.224	2.222
Pt–P	2.405	2.406	2.402	2.403
Pt–C(1)	2.027	2.028	2.026	2.029
Pt–C(2)	2.047	2.047	2.047	2.046
C(1)-Pt-C(2)	92.2	92.2	92.3	92.3
C(1)-Pt-N	171.7	171.7	171.8	171.8
C(1)-Pt-P	88.3	88.2	88.5	88.6
P-Pt-C(2)	179.4	179.5	179.0	179.1
P-Pt-N	99.9	100.0	99.6	99.6
C(2)-Pt-N	79.5	79.6	79.5	79.6

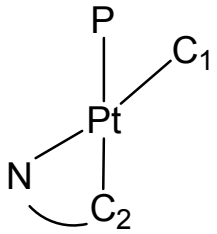

Table S43. Selected bond distances (Å) and angles (deg) of the optimized structures of Complexes **3** in the ground state.

	3a(calc.)	**3b**(calc.)	**3b**(exp.)	**3c** (calc.)
Pt–N	2.121	2.129	2.106	2.153
Pt–P	2.292	2.292	2.224	2.297
Pt–C	2.016	2.034	2.013	2.043
Pt–X	2.169	2.470	2.394	2.835
C-Pt-X	170.7	171.5	171.3	170.6
C-Pt-N	81.3	80.7	81.2	80.3
C-Pt-P	98.9	97.9	96.0	96.5
P-Pt-X	90.3	90.6	92.2	91.1
P-Pt-N	176.1	178.4	176.7	175.2
X-Pt-N	89.4	90.8	90.6	92.3